Contact mechanics and elements of tribology

Lecture 7.

Wear and Fretting

Siegfried Fouvry & Henry Proudhon

Contact : siegfried.fouvry@minesparis.psl.eu

MINES ParisTech, PSL University, Centre des Matériaux, CNRS UMR 7633, Evry, France

@ Centre des Matériaux
February 10, 2021

Outline

1. Wear
   - Adhesive wear
   - Abrasive wear
   - Chemical wear
   - Experimental testing
2. Fretting
   - Basics
   - Fretting wear
   - Experimental determination of fretting crack initiation
   - Numerical analysis of fretting initiation and propagation
   - Fretting fatigue
3. Modelling fretting taking into account the contact gradient
4. Outlook : insight from numerical models

Outline

1. Wear
   - Adhesive wear
   - Abrasive wear
   - Chemical wear
   - Experimental testing

Definition

Wear is a very general term which is defined as the degradation of the contact surface of a material in service. These degradations can be due to multiple factors, and it is now common to separate wear into 4 distinct families :

- adhesive wear ;
- abrasive wear ;
- chemical wear (corrosion) ;
- wear by contact fatigue.

We will first describe the first three types of wear, wear by contact fatigue will be discussed in more detail in section 2.

Contents

Adhesion of two solids in contact

Creation of strong bonds leading to the formation of junctions between the two materials at the level of asperities in contact. The stresses at the level of the asperities are generally high enough to generate local plastic deformations and the creation of adhesive interfacial bonds.

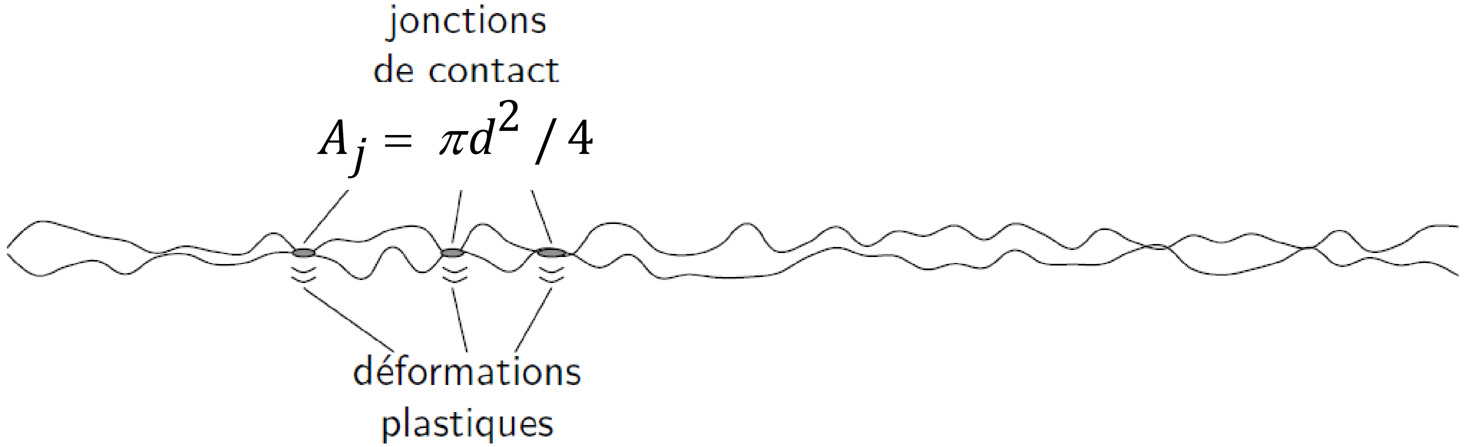

Adhesion index

The adhesion index provides information on the propensity for two materials to adhere to each other if they are brought into contact.
It is expressed as a function of the effective Young's modulus E^*, the average radius of curvature of the asperities R, the standard deviation of the height distribution of the asperities σ and the adhesive work W_{ad} :

$$\alpha = \frac{E^*}{W_{ad}} \left(\frac{\sigma^3}{R} \right)^{1/2}$$

In practice, if $\alpha \leq 5$, risks of adhesion are important.

Plasticity index

The plasticity index provides information on the risk of plastic deformation of a rough surface subjected to a load P :

$$\psi = \frac{P}{H}\left(\frac{\sigma}{R}\right)^{1/2}$$

For $\psi \leq 0{,}6$ the deformation of the surface remains essentially elastic, while for values greater than unity, the deformation will be mainly plastic.
This index is used to predict the running-in periods, where a transition from the plastic domain to the elastic domain is observed.

Adhesive wear

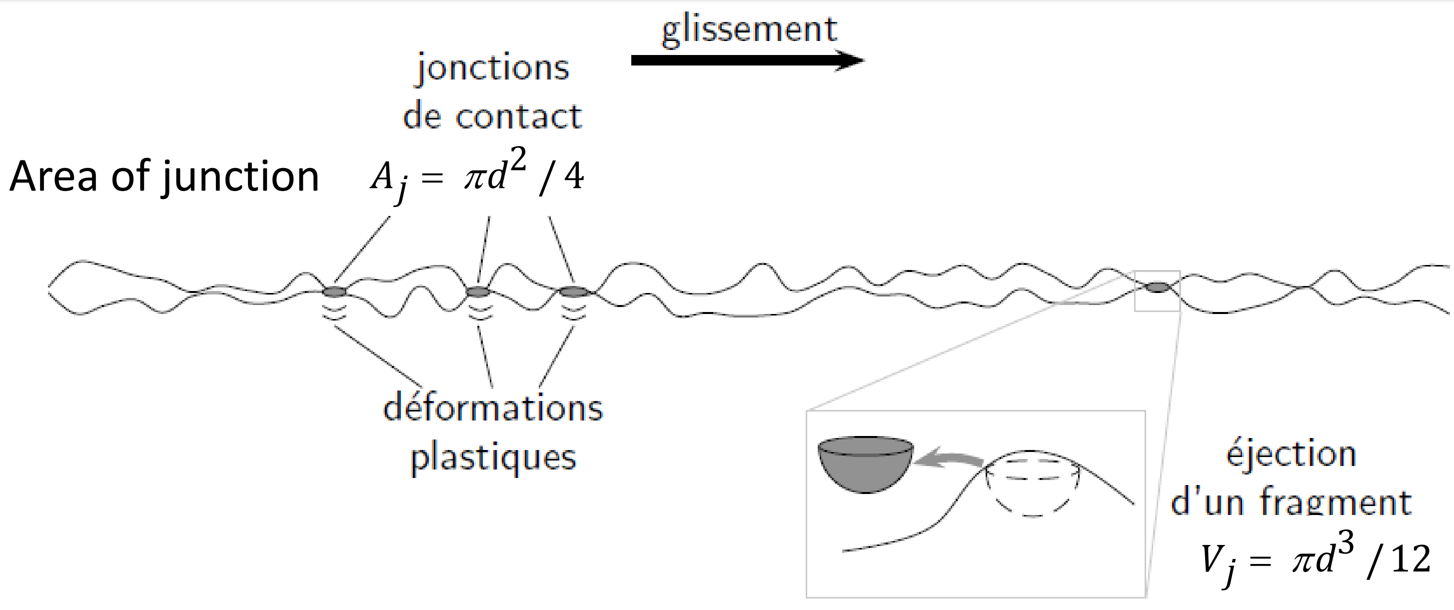

- In the presence of adhesion ($\alpha \leq 5$) and if sliding is imposed, wear will occur.
- Some junctions can break and lead to the formation of a material particle, which is usually transferred to the surface of the contacting body ; this particle can then be ejected later as debris.
- Adhesive wear is directly related to the real contact area between the two bodies $\approx P/H$.

Archard Model

Mean area of a Junction : $A_j = \pi d^2 / 4$

Volume of a broken a Junction: $V_j = \pi d^3 / 12$

Real contact area (plastic accommodation) = Normal force P / Material Hardness H:

$A_r = P / H$

Number of junction at a given time $n = \dfrac{A_r}{A_j} = (P / H) / (\pi d^2 / 4)$

Considering a displacement Δl, Archard supposes that each junction is broken after a distance d. Thus, N junctions will have formed such that :

$$N = n \cdot \frac{\Delta l}{d} = 4 \cdot \frac{P}{H} \cdot \frac{\Delta l}{\pi d^3}$$

Archard Model

J. F. Archard, Contact and rubbing of flat surfaces, Journal of Applied Physics, p 981-988 (1953).

If K is the probability for a junction to give rise to the transfer of a particle, the used volume is expressed by $\Delta V = KN\pi d^3/12$.

i.e. $$\Delta V = K \cdot N \cdot V_j = K \cdot N \cdot \frac{\pi d^3}{12}$$

$$\Rightarrow \Delta V = K \cdot N \cdot \frac{\pi d^3}{12} = K \cdot 4 \cdot \frac{P}{H} \cdot \frac{\Delta l}{\pi d^3} \cdot \frac{\pi d^3}{12} = \frac{K \cdot P \cdot \Delta l}{3 \cdot H}$$

$$\Delta V = \frac{K \cdot P \cdot \Delta l}{3 \cdot H} \Rightarrow \boxed{V = \frac{K \cdot P \cdot S}{3 \cdot H} \propto P \cdot S}$$

S : Total sliding distance

The wear volume is proportional of the product of the normal force (P) by the Sliding distance (S) and inversely proportional to the Hardness !

K is called the wear coefficient and allows to compare various materials with each other for their resistance to wear. The higher the value of K, the greater the wear.

Understanding the wear coefficient K

K represents the fraction of the contact junctions which will produce wear fragments.

- $K = 1$: Every junction involved in the friction process produces a wear fragment.
- $K = 0.1$: One tenth of the friction junctions produce wear fragments. For clean gold surfaces K is between 0.1 and 1. For clean-copper surfaces K is between 0.1 and 0.01. Clean gold surfaces wear about ten times more rapidly than clean copper surfaces.
- $K = 10^{-7}$: One contact junction in ten million produces a wear fragment.

Values of some wear coefficients

The following table presents values of wear coefficients for different combinations of materials in contact[1]. It should be noted that the presence of a lubricant allows the coefficient of wear to be reduced significantly.

Materials in contact	Wear coefficient K
Zinc on Zinc	$160 \cdot 10^{-3}$
Copper on Copper	$32 \cdot 10^{-3}$
Stainless steel on Stainless steel	$21 \cdot 10^{-3}$
Copper on Low carbon steel	$1,5 \cdot 10^{-3}$
Low carbon steel on Copper	$0,5 \cdot 10^{-3}$
Bakelite on Bakelite	$0,02 \cdot 10^{-3}$

M. Shaw M, *Friction and Wear*, p 657-673, Addison Wesley, Reading MA (1966).

Contents

Abrasive wear

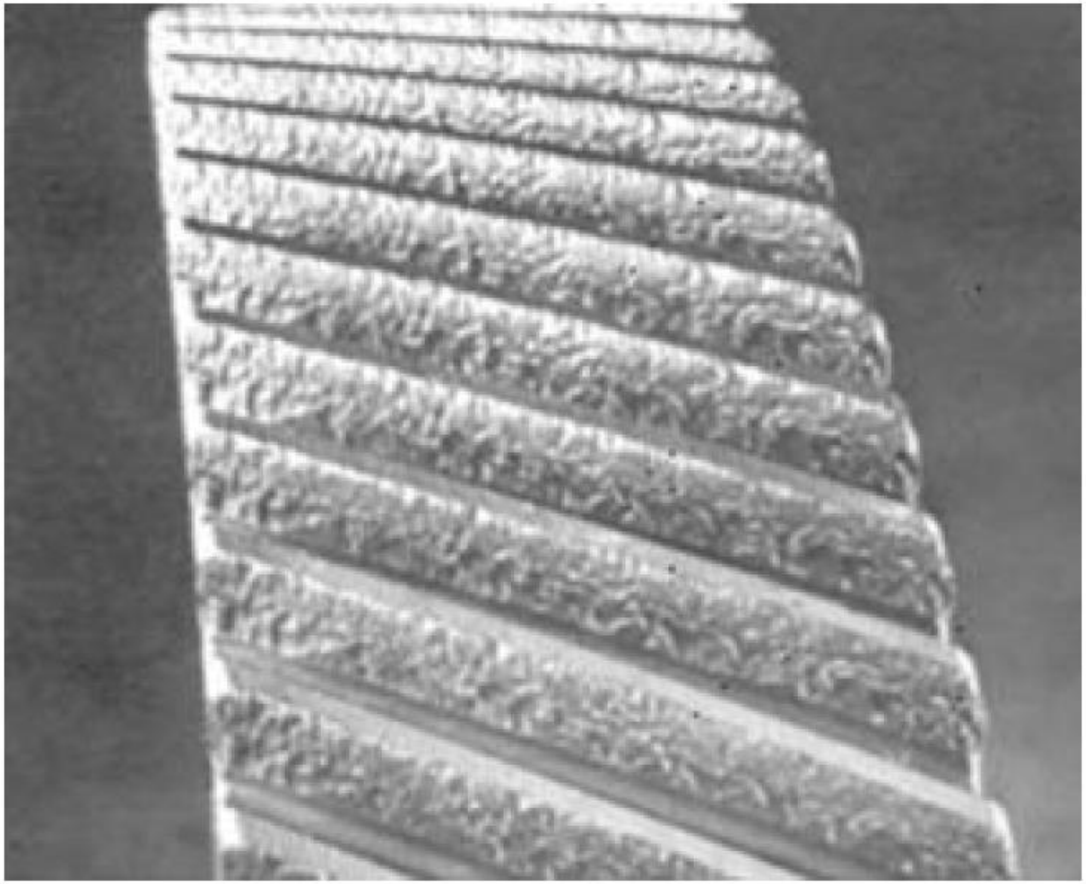

Abrasive wear description

- A hard surface penetrates a softer surface ;
- the relative displacement of surfaces causes degradation.

two-bodies wear when the two materials in contact have very different hardnesses

three-bodies wear when small, very hard particles are located between the two materials (introduced intentionally, as in the case of polishing, or generated by the first phases of two-body wear or tribochemical reaction).

→ Wear manifests itself by the creation of plastic grooves on the surface of the worn material and the possible ejection of particles of material.

Prediction of the wear volume ΔV

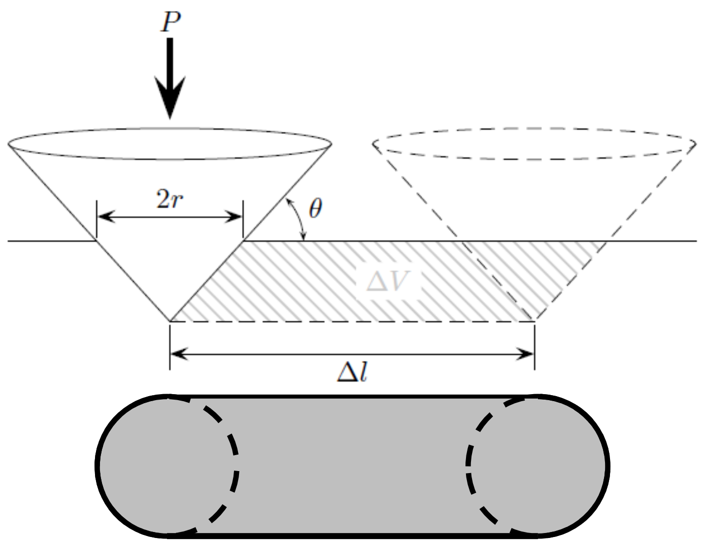

Conical particle penetrating the softer material, displaced by a distance Δl.
The volume of the groove created by the displacement of the conical particle is expressed by $\Delta V = r^2 \tan\theta \Delta l$, while the indentation pressure is directly related to the hardness H of the softer material and at the contact area : $P = \pi r^2 H$. We can therefore write :

$$\frac{\Delta V}{\Delta l} = \frac{\tan\theta}{\pi}\frac{P}{H} \Rightarrow V = \frac{\tan\theta \cdot P \cdot S}{\pi \cdot H} \propto P \cdot S$$

S : Total sliding distance

Prediction of the wear volume ΔV

$$\frac{\Delta V}{\Delta l} = K' \frac{P}{H}$$

This law is globally of the same form as Archard's law except for the multiplicative coefficient. Compared to adhesive wear, wear coefficients depend essentially on the geometry of the abrasive particles and are more in the order of 10^{-3} for three-bodies wear and 10^{-2} for two-bodies wear. Two-bodies wear is therefore much more dangerous, with the third body playing the role of a solid lubricant.

Contents

Tribochemical wear

Contact degradations in the presence of a reactive environment are qualified as tribochemical wear. Damage is dominated by chemical reactions occurring between the contact surfaces and / or the external environment. These phenomena interact with mechanical stresses which can sometimes facilitate reactions.

If the medium is corrosive, we can also observe a phenomenon of tribocorrosion activated by contact stresses in the same way as damage by stress corrosion. The deterioration of wear is then greatly increased.

The corrosive wear volume W is normally defined by the following equation [14]:

$$W = M_0 + C_0 + \Delta W \quad (1)$$

where M_0 is the pure mechanical wear volume, C_0 is the pure (static) corrosion volume, and ΔW is the synergistic factor. The dynamic corrosion factor W_d on a fresh surface is written as

$$W_d = C_0 + \Delta W \quad (2)$$

The synergistic factor ΔW involves both ΔC_M and ΔM_C. Here, ΔC_M is the mechanical-assisted corrosion factor, indicating the corrosion volume on the fresh surface exposed by mechanical factors. Moreover, ΔM_C is the corrosion-assisted mechanical wear, describing the effect of oxide film removal on the wear scar. Depending on the condition, these oxide films could either reduce wear by lubricating or accelerate wear by abrasion. Therefore, the corrosive wear volume is expressed as follows [14–17]:

$$W = M_0 + W_d = M_0 + C_0 + \Delta C_M + \Delta M_C \quad (3)$$

Schematic diagrams of these wear factors are shown Fig. 1.

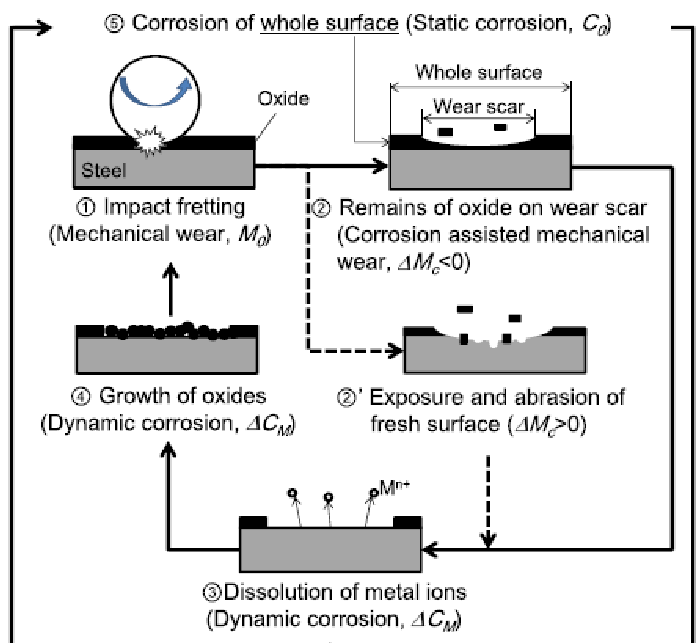

Tribochemical wear

The formation of oxides under these conditions (tribo-oxidation) can have either beneficial or harmful effects on the mechanical strength of the parts :

- the oxide layer formed can limit mechanical stresses, by lowering the coefficient of friction or by adaptated plasticity (plastic shakedown) ;
- if this layer fractures under the action of mechanical contact stresses, it is quickly eliminated. The action depends on whether the debris will effectively play the role of third body by lubricating the contact. If this is not the case (hard and abrasive debris) the damage can quickly become catastrophic.

Contents

Tribometers

Schematic illustration of some sample configurations used in simulation of dry or partially lubricated sliding contacts :

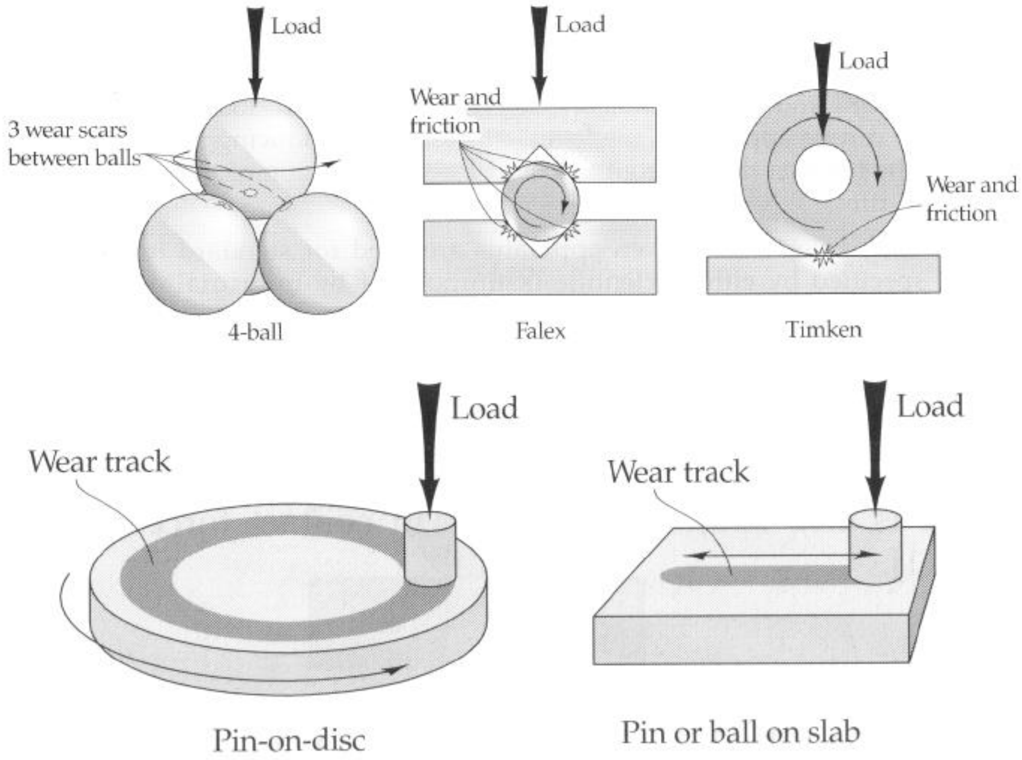

Pin on disk tribometer standards

DIN 50 324 Testing of friction and wear

ASTM G 99 - 95a Standard test method for wear testing with a Pin-on-Disk apparatus

ASTM G 133 - 95 Standard test method for linearly reciprocating ball-on-flat at sliding wear

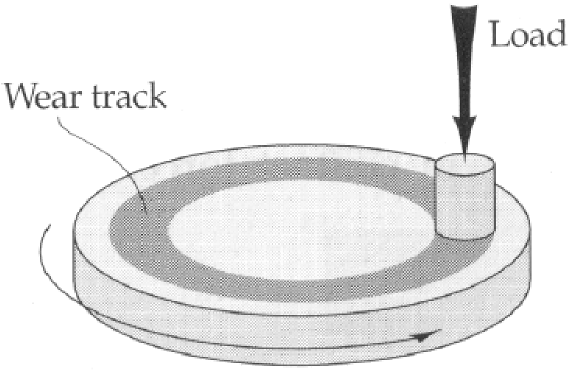

Pin-on-disc

Comonly used parameters in the characterisation of tribological contacts

Operating parameters

- Load
- Sliding speed
- Sliding distance

Lubrication parameter

- Viscosity
- Flow rate
- Thermal conductivity
- Acidity
- Boiling point
- Solidification point

Material parameters

- Hardness
- Toughness
- Melting point

Environmental parameters

- Relative humidity
- Local air pressure
- Radiation level

Tribometers at CdM

Pin on disc tribometer

- CSM company
- rotating specimen vs fixed pin
- environmental control chamber

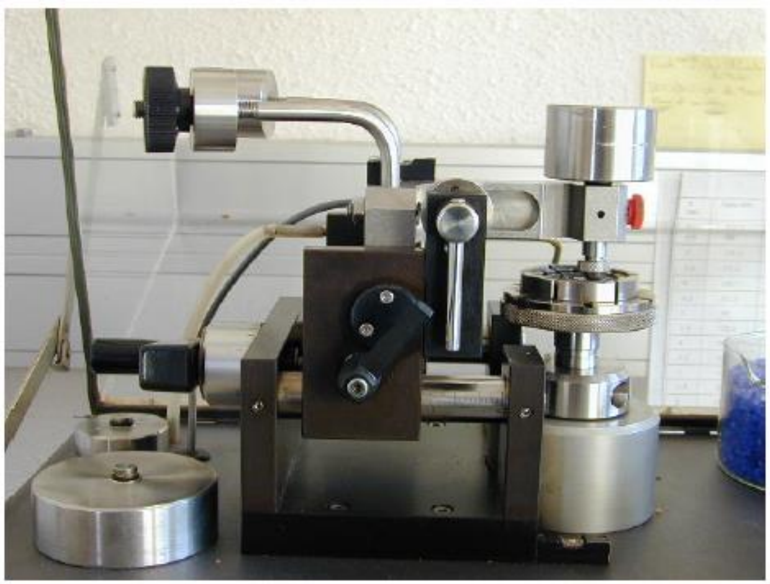

High load UMT TriboLab

- CETR (now Brucker) company
- reciprocating sliding
- motorized 500 N normal load

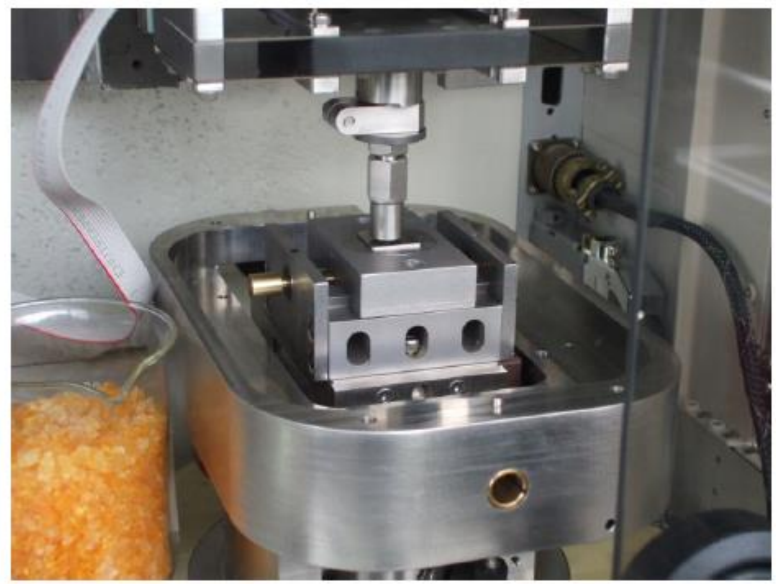

Scratch test

Investigation of the phenomena occuring along the scratch deformation : cracking, spallation, delamination or bulking.

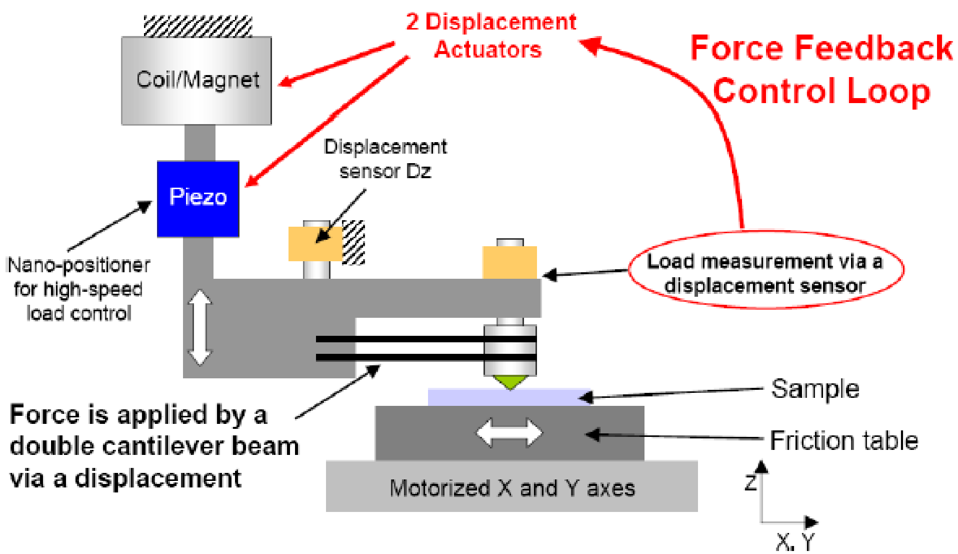

Quantify :

- Scratch resistance
- Adhesion of Coatings
- Friction Coefficient
- Viscoelastic properties
- Wear Testing
- Conventional Hardness

Scratch test to quantify coatings adhesion to substrate

→ scratching a surface with an indenter or ball to characterize the critical loads (L_C) at which the coating failure failure occurs.

www.iphoneincanada.ca

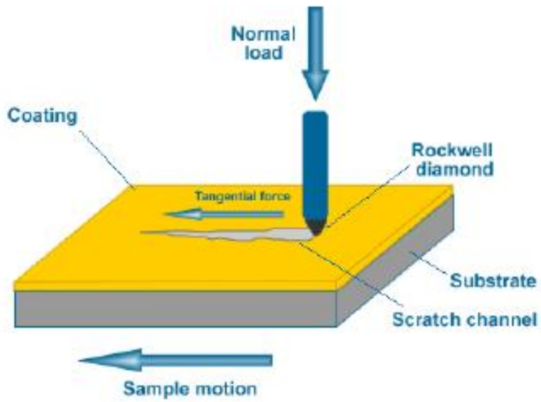

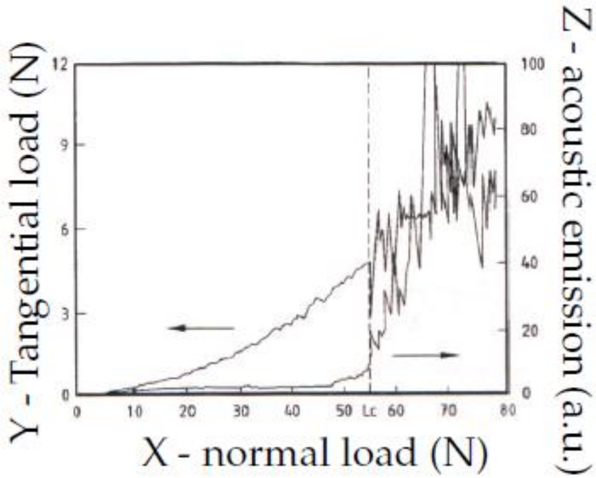

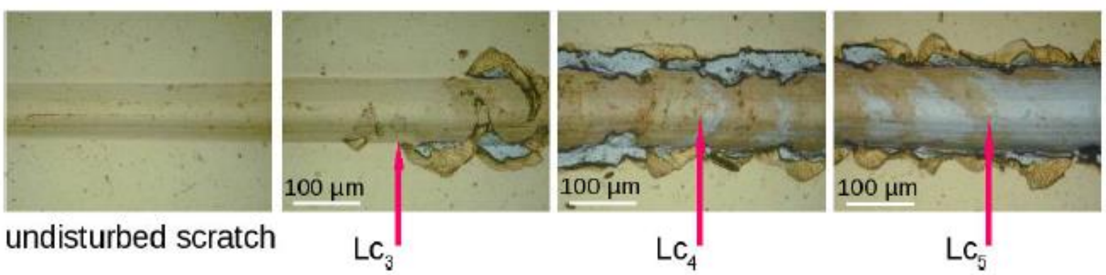

Standard EN 1071-3

Three different scratching procedures :

- Progressive load scratch test (PLST)
  - loading rate 100 N/min
  - lateral displacement speed 10 mm/min

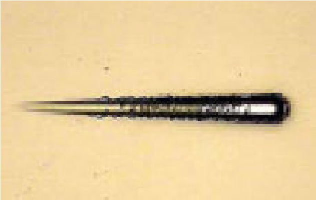

- Constant load scratch test (CLST)
  - loading rate 100 N/min
  - lateral displacement speed 10 mm/min
  - load step 1/5 of L_C

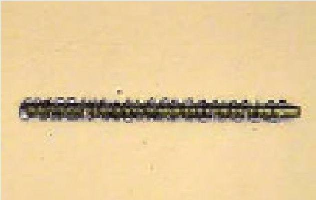

- Multipass scratch test (MPST)
  - repeated scratching under a constant sub-critical load within the same scratch track
  - lateral displacement speed 1operating parameter same as for CLST
  - load 1/2 of L_C
  - number of scratches until failure

Contents

Context and challenges

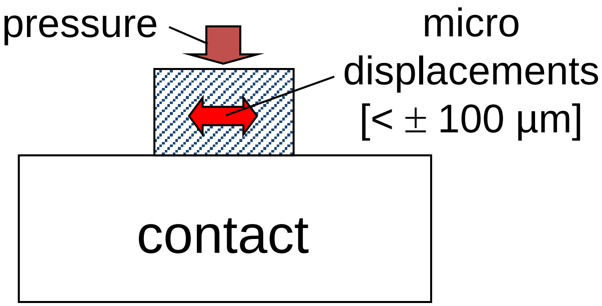

electrical connectors

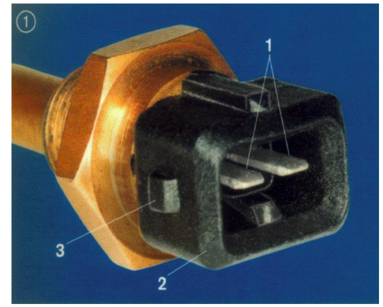

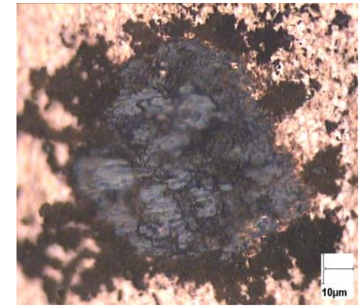

[Bosh]

bridge cables

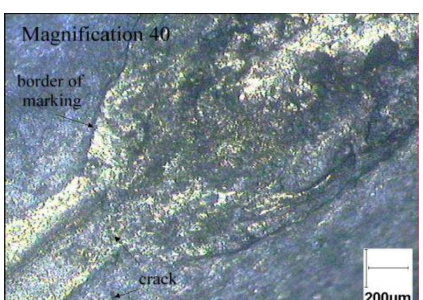

blade / disk contacts in turbine engine

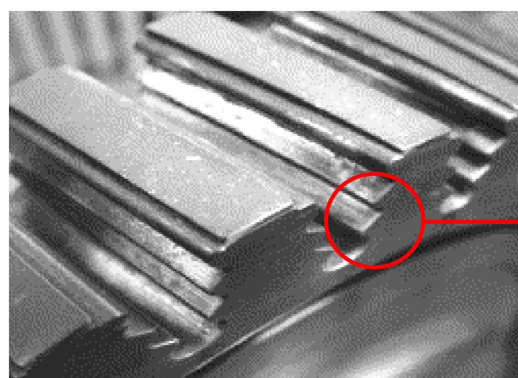

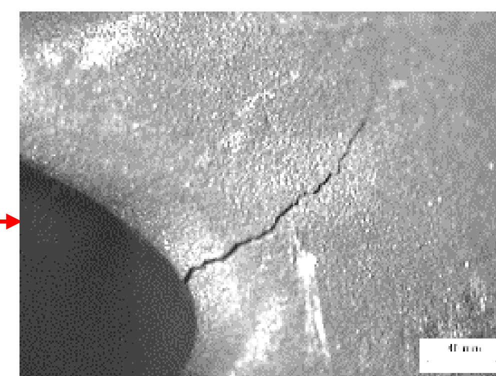

[M. Park et al.]

Contact configurations

Very complex real contact geometries → simplification of the geometry for laboratory testing.

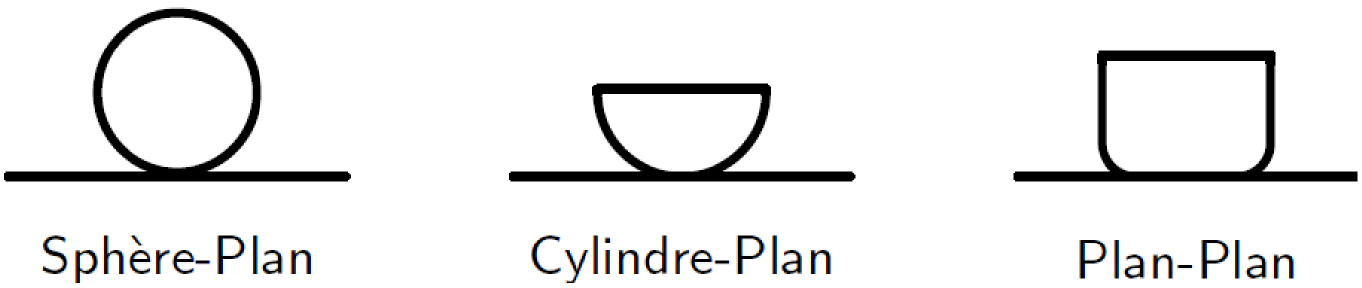

- The sphere-plane and plane-plane configurations are often used to study the kinetics of fretting wear ;
- rather, the cylinder-plane configuration is used to study fretting cracking.

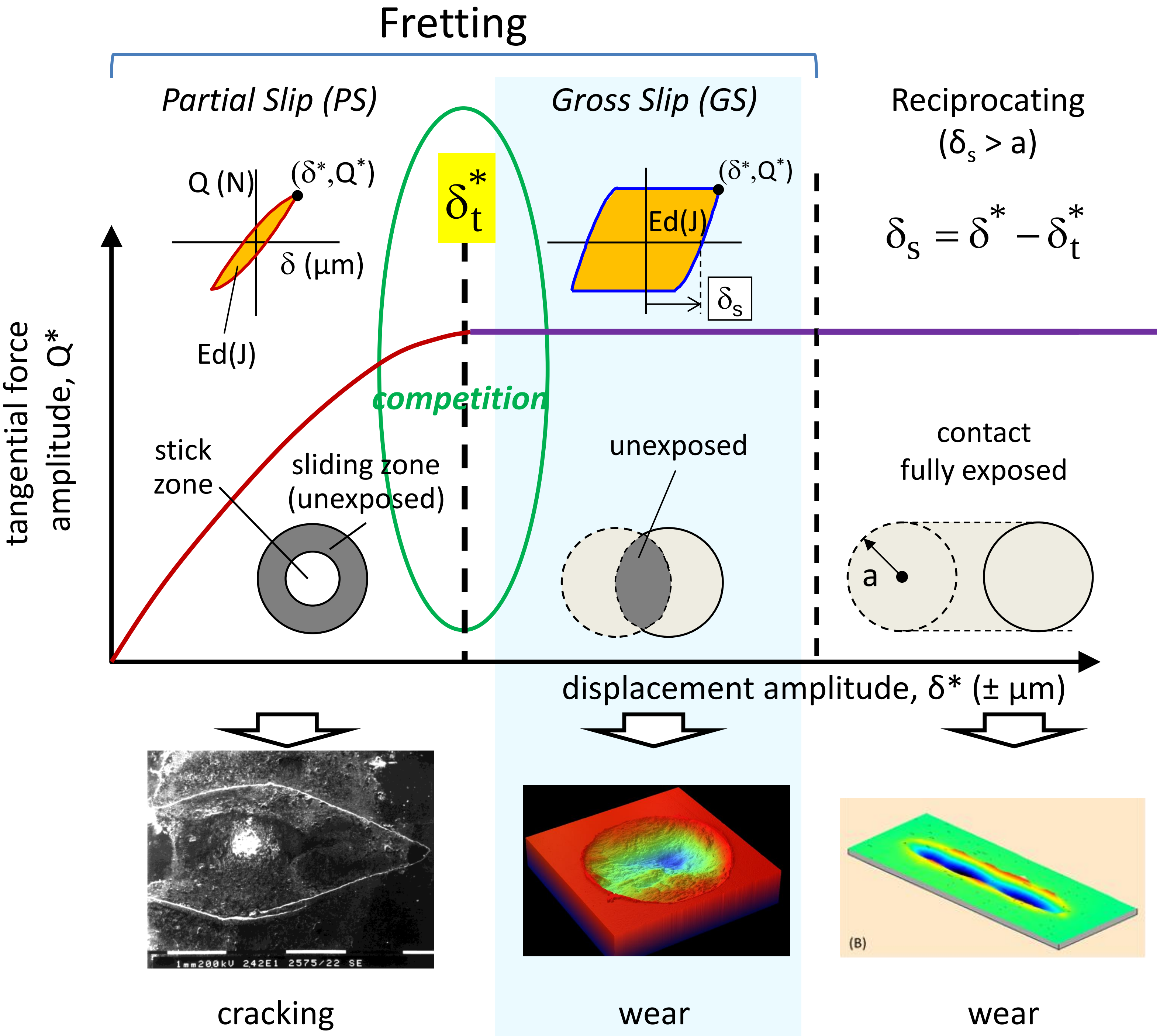

Fretting
Partial Slip (PS)
Gross Slip (GS)
Reciprocating
(δ_s > a)
Q (N)
(δ^*,Q*)
δ (µm)
Ed(J)
δ_t^*
Ed(J)
(δ^*,Q*)
δ_s
$\delta_s = \delta^* - \delta_t^*$
tangential force amplitude, Q*
competition
stick zone
sliding zone (unexposed)
unexposed
contact fully exposed
a
displacement amplitude, δ* (± µm)
cracking
wear
wear

Fretting Wear

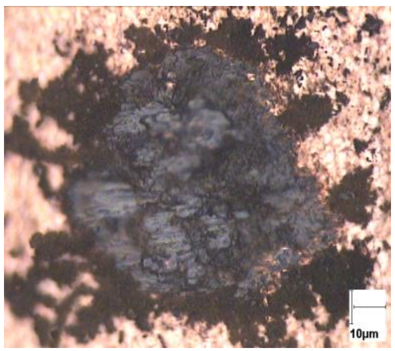

Fission Reactors

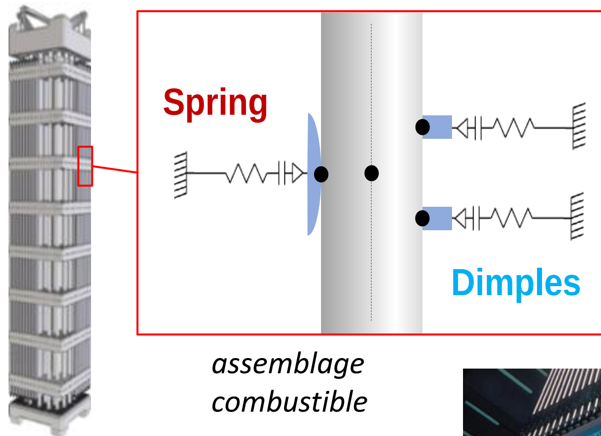

assemblage combustible

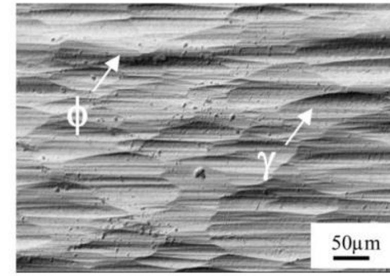

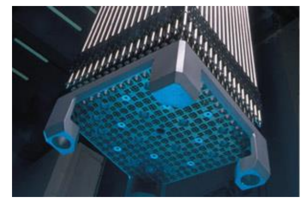

Fretting Wear

Fusion Reactors

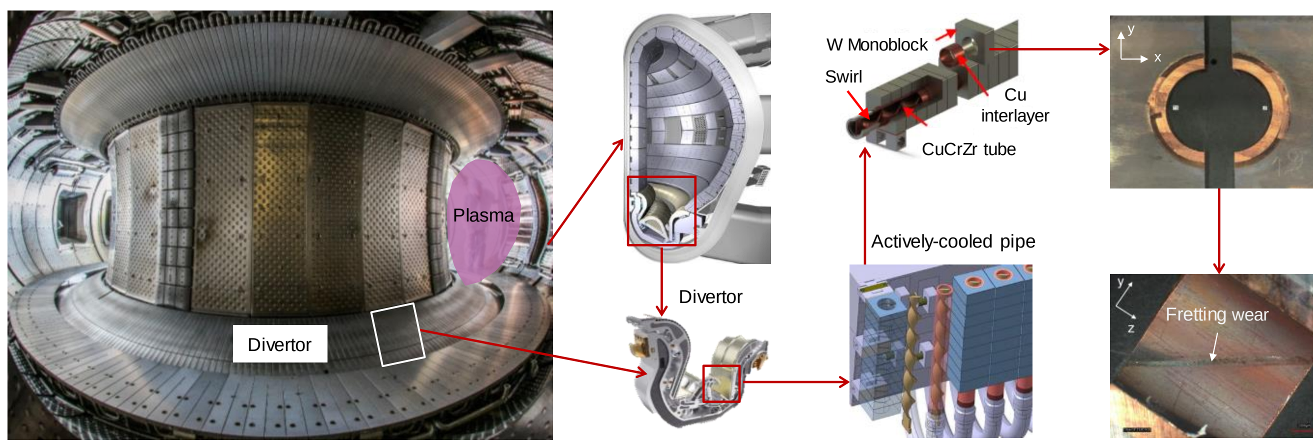

Friction energy wear approach

Sum the area of the fretting loop

$$\Sigma Ed$$

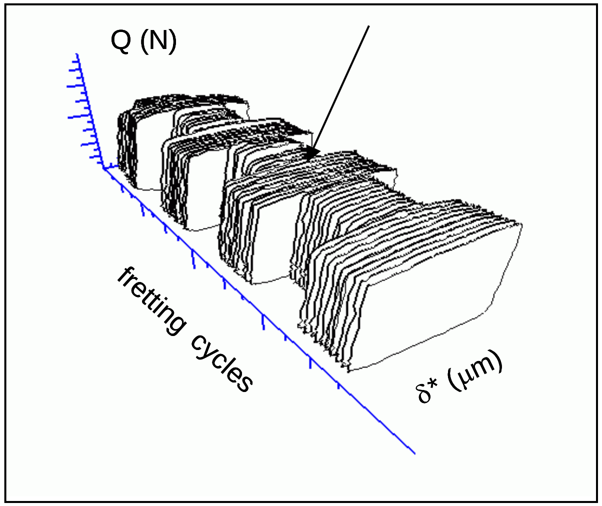

Σ Accumulated Friction work)

$$\Sigma Ed$$

Σ transformations & degradations

$$V = \alpha \times \Sigma Ed$$

Wear Volume

α : energy wear coefficient

Wear volume

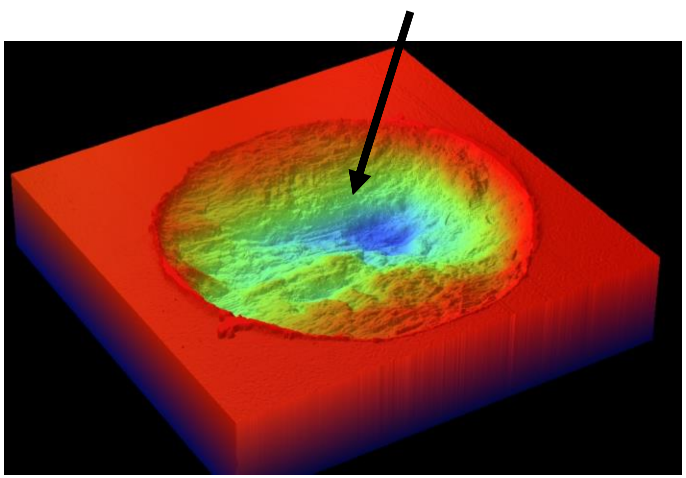

$$V = V_{plan} + P_{pion}$$

S. Fouvry, Ph. Kapsa, H. Zahouani, L. Vincent, "Wear analysis in fretting of Hard coatings through a dissipated energy concept", Wear 203-204 (1997), p. 393-403

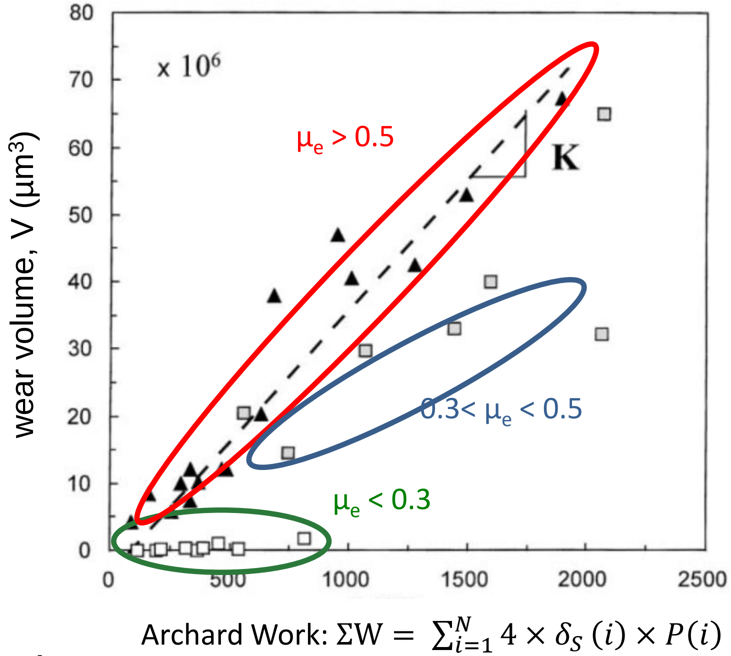

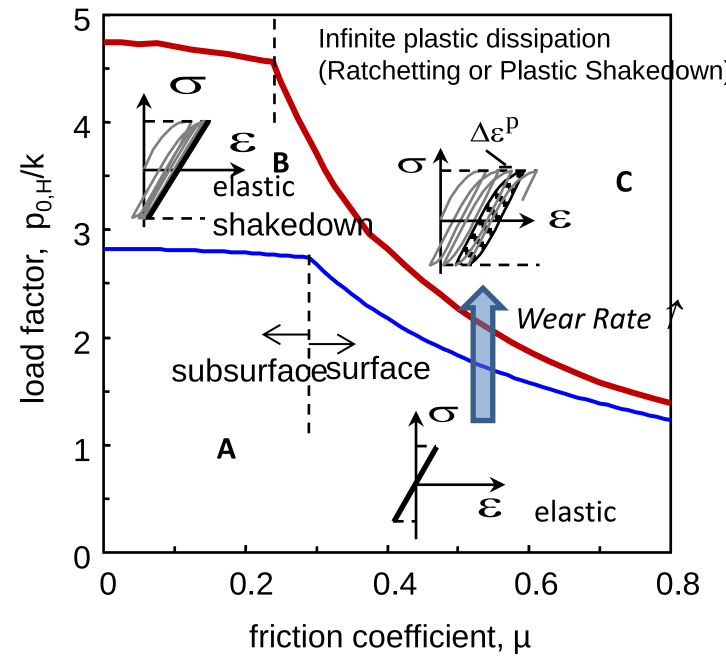

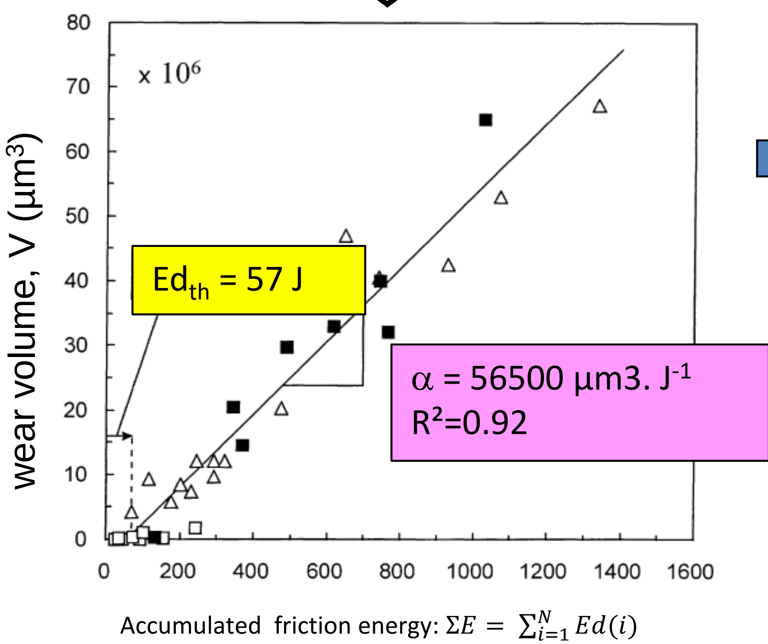

Using friction energy the Wear volume correlation Is more stable (i.e. linear)

⇒ Take into account the coefficient of friction !

⇒ If CoF constant

Archard = Energy wear approach

Variable sliding amplitude conditions : Abrasive Wear Process

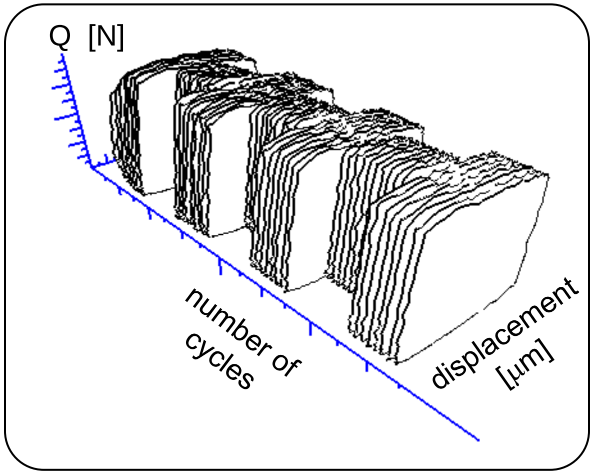

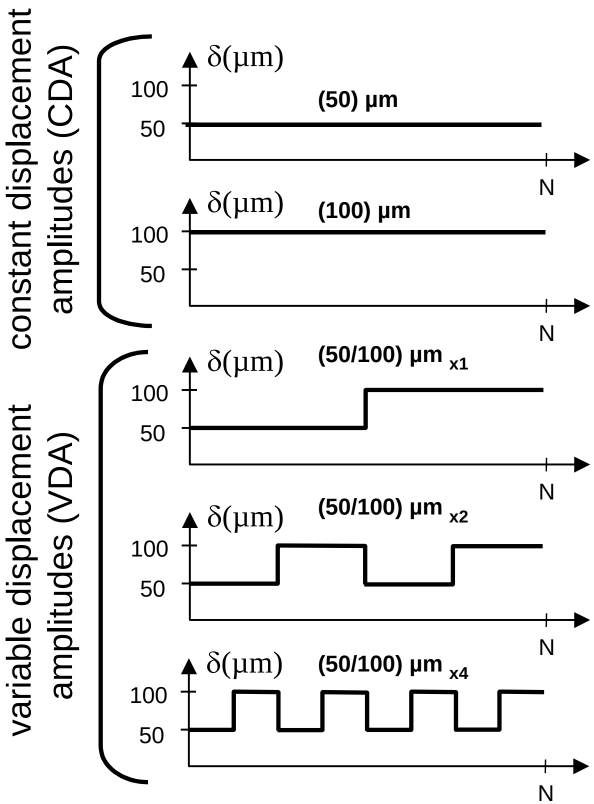

Ceramic contacts

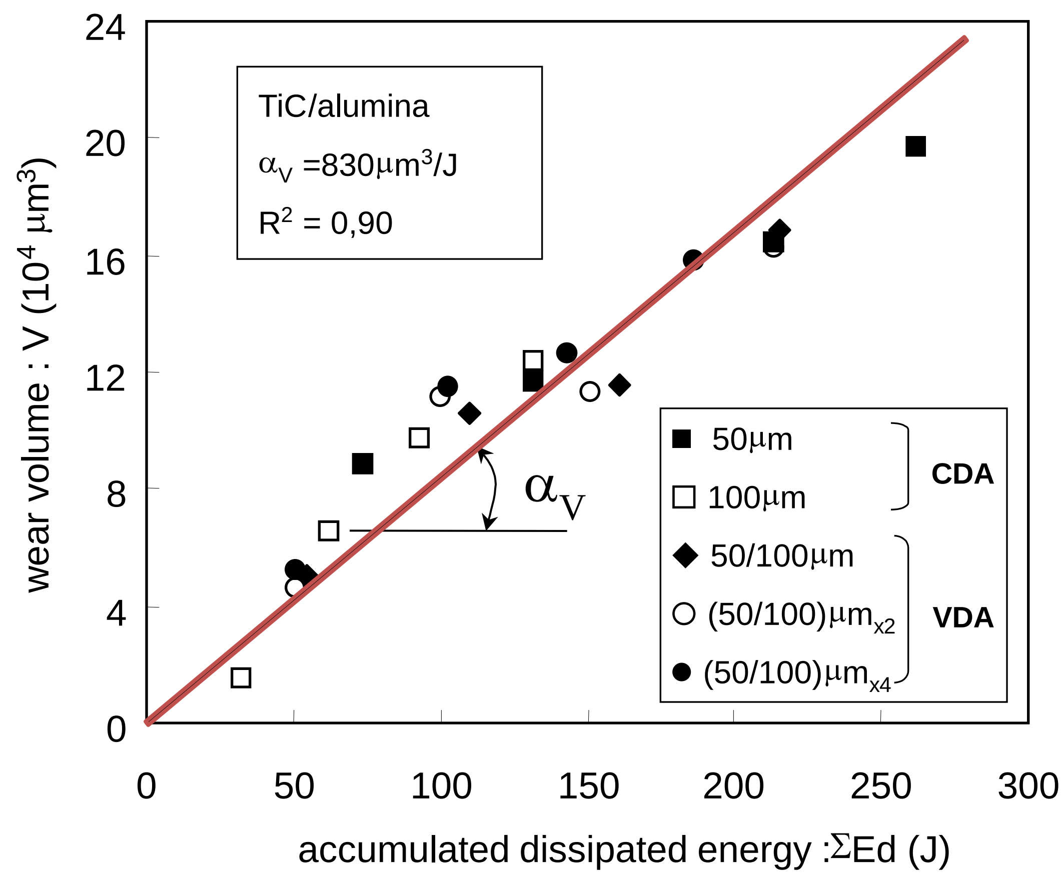

Stability of the energy wear approach under variable sliding amplitude conditions ?
if a similar Fretting Wear process is activated an additive approach can be considered.

Energy as an activating factor of wear phenomena (Energy balance)

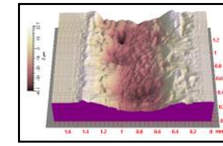

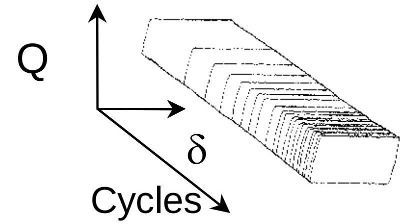

Major dissipating processes

Dissipated energy (Σ cycle area)

Transformation of the microstructure	*Tribochemical transformations*	*Third body*	*Heating*
Plastic deformation, TTS transformation, Fracturation	Oxidation, Hydratation, etc...	Aggregation, Transformation, Debris flow,...	Caloric transfers, Flash temperatures

Less than 10%

Less than 1%

Σ Transformations and degradations

Material loss, Debris flow: WEAR

Wear

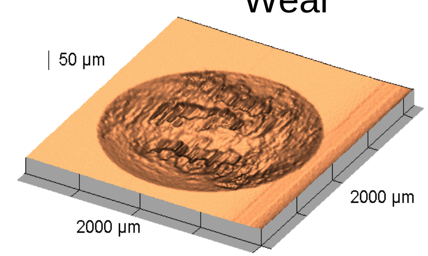

Time duration of surface coating : A local approach

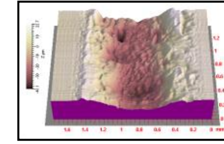

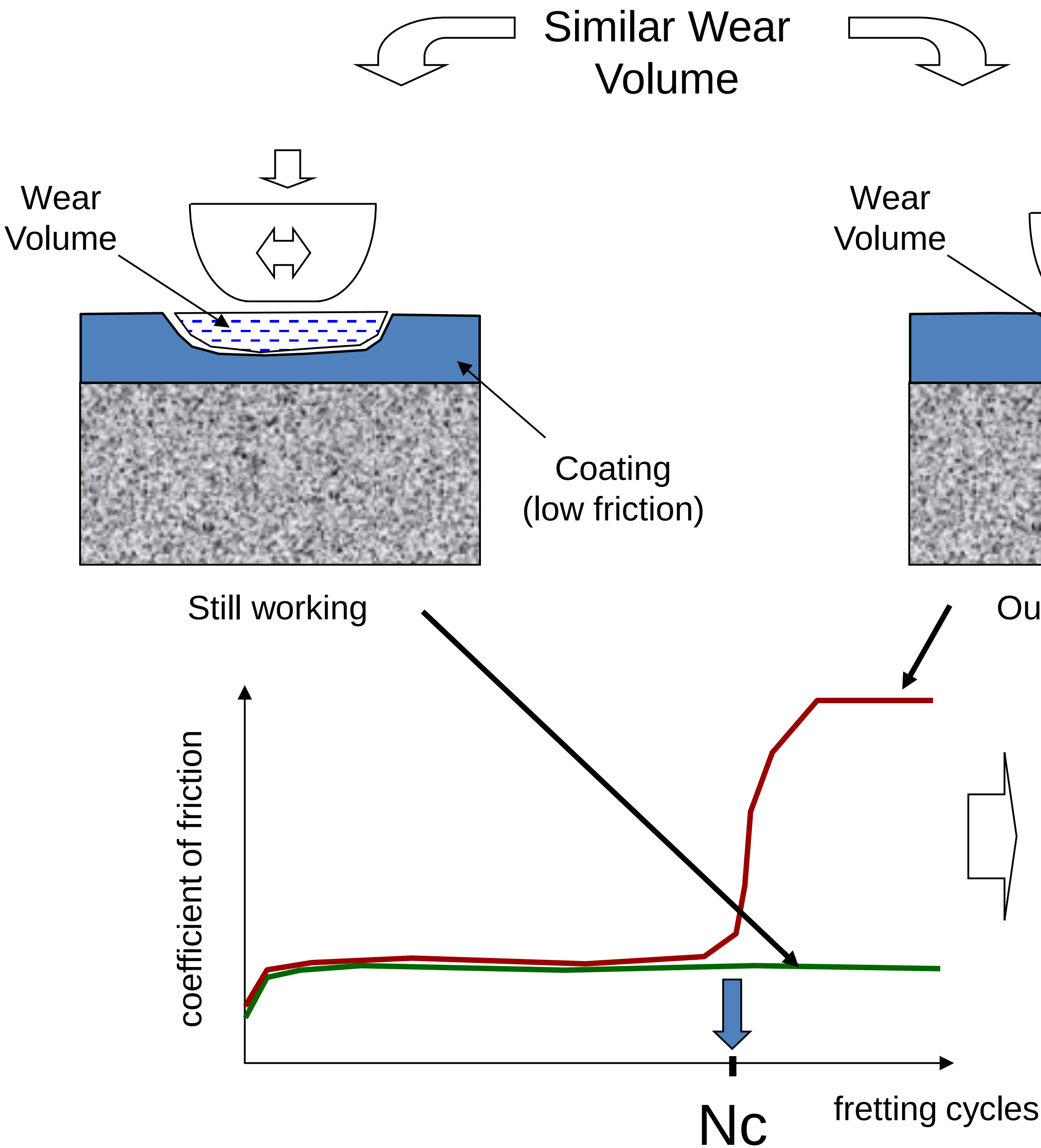

- Introduction of a coating endurance concept.

-Request a local analysis of wear : Replace the wear volume description by a wear depth extension.

Prediction of the coating endurance : Local energy approach

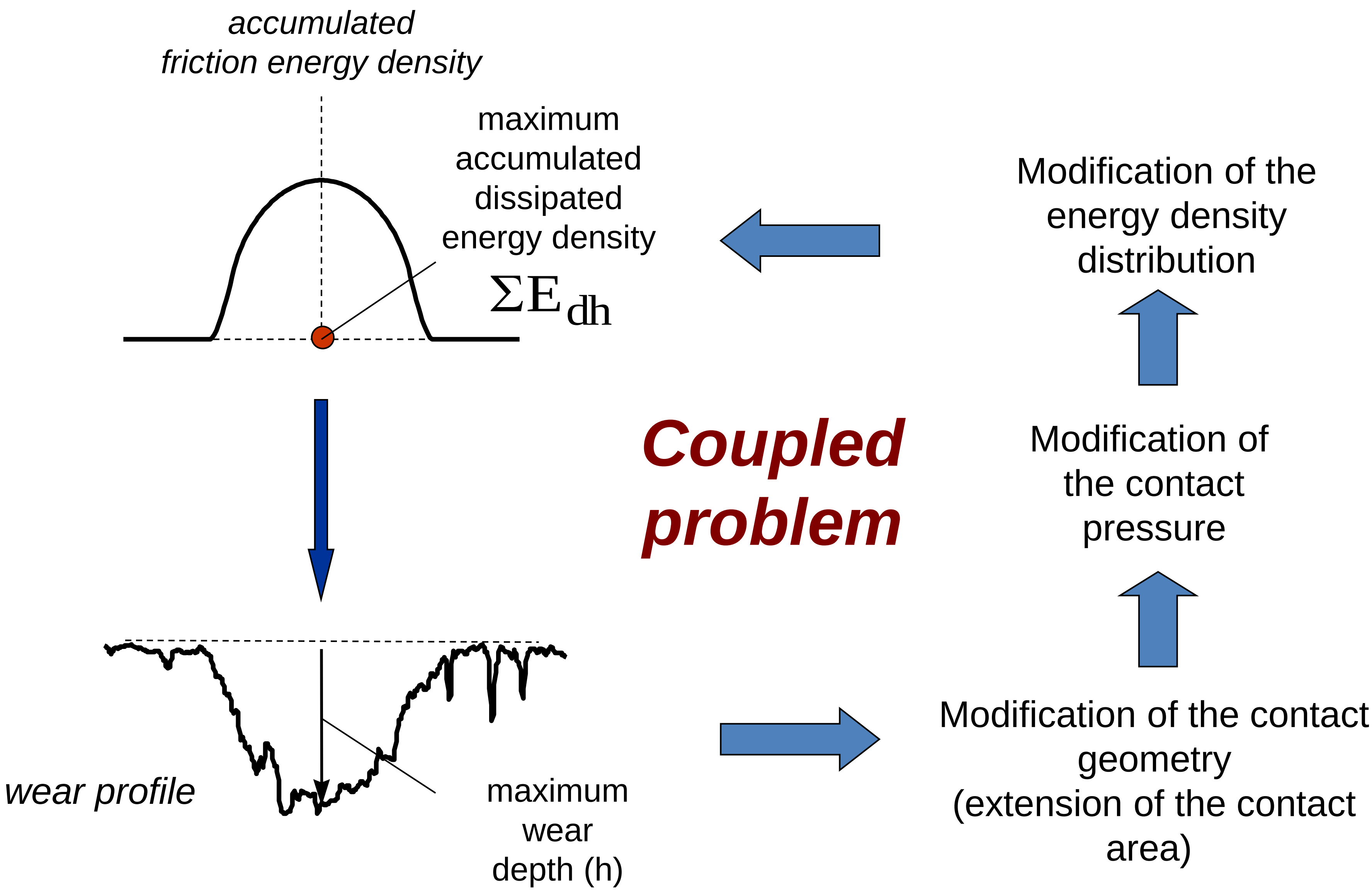

Development of a couple FEM modelling (Wear Remeshing)

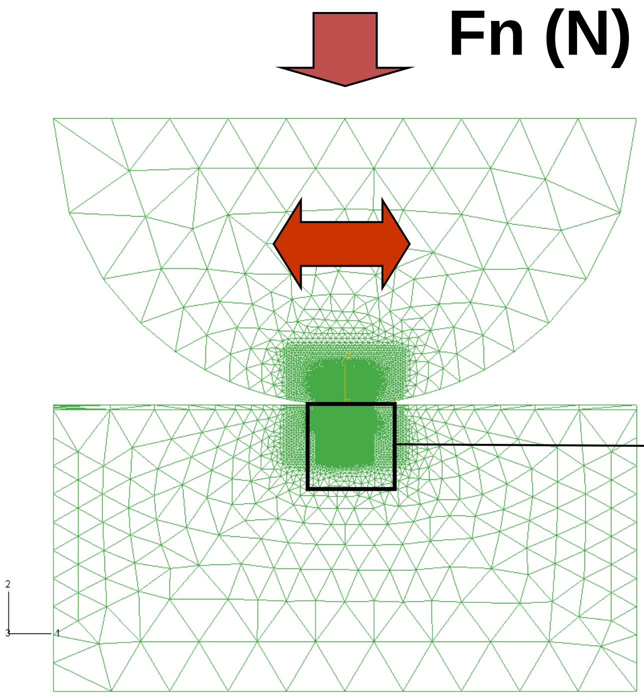

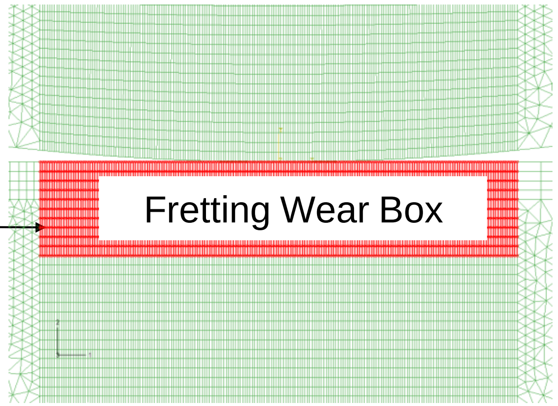

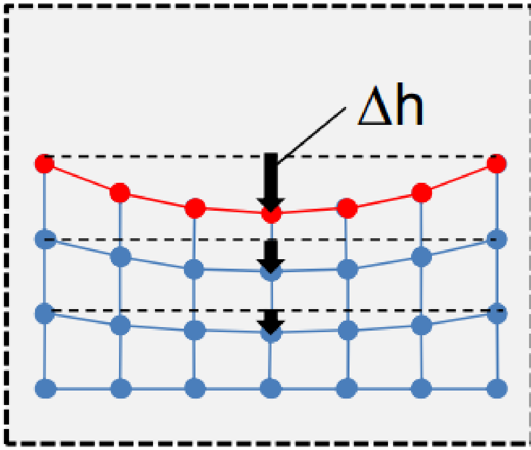

2D cylinder/plane configuration
TA6V/TA6V

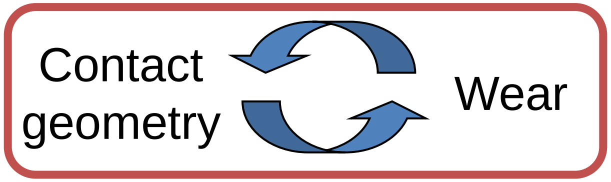

Coupled Abaqus - Mathlab code

- Computation of the energy density on the top surface
- Integration of the local wear $\Delta h = \alpha \,.\, \Delta Edh$
- Modification of the contact geometry (*Wear Remeshing*)

C. Mary, S. Fouvry, "Numerical prediction of fretting contact durability using energy wear approach: Optimisation of finite-element model", Wear (2007); 263(1-6): 444-450

Development of a couple FEM modelling

2D cylinder / plane configuration
TA6V/TA6V (R=10 mm, P=133 $N.m^{-1}$, δ= +/- 75 µm)

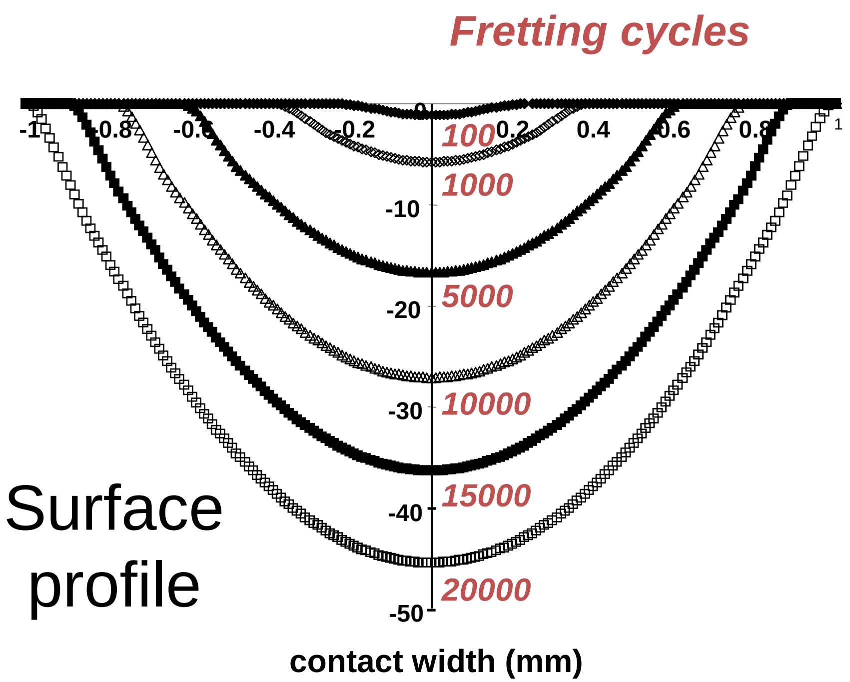

Surface energy density distributions (J/mm²)

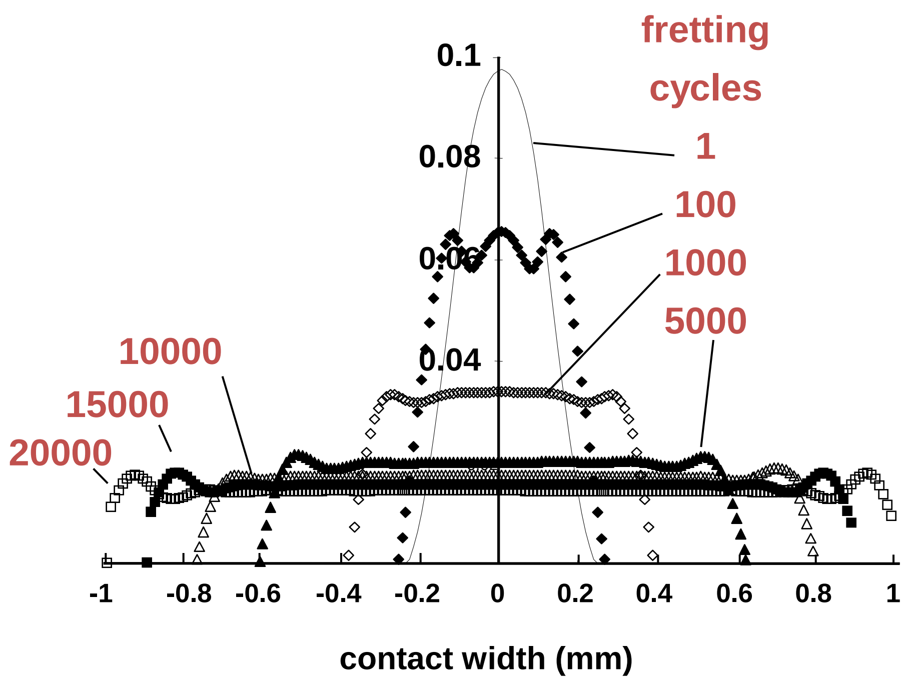

- After less than 100 cycles an homogenous pressure field can be approximated !!

Comparison with experiments (Ti-6AL-4V)

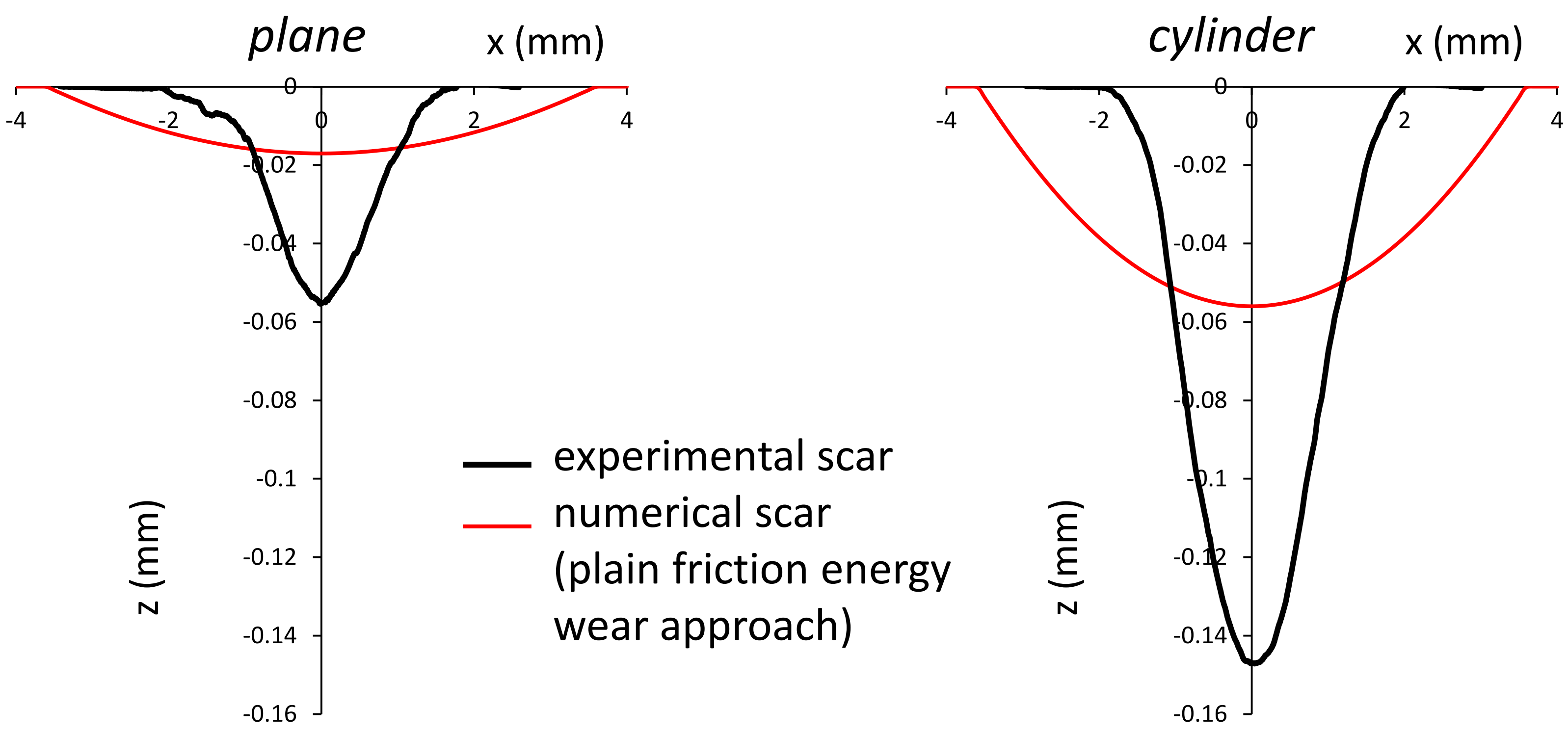

Under estimation of the maxiumum wear depth !
=> Debris layer !

Upgrading of the numerical Wear Modeling to consider the third body layer

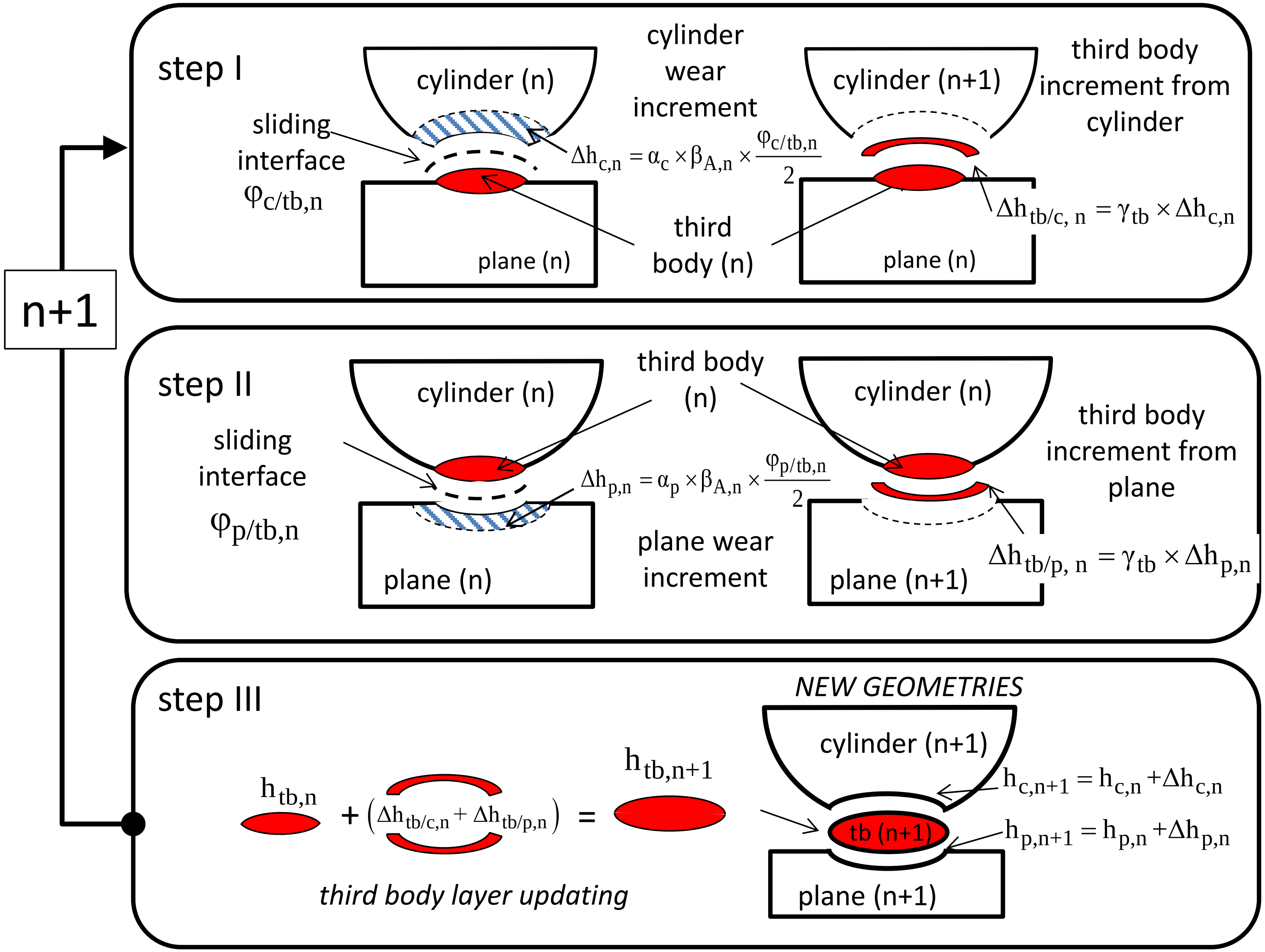

P. Arnaud, S. Fouvry, A dynamical FEA fretting wear modeling taking into account the evolution of debris layer, Wear, Volumes 412–413 (2018) 92-108

wear simulation with third body

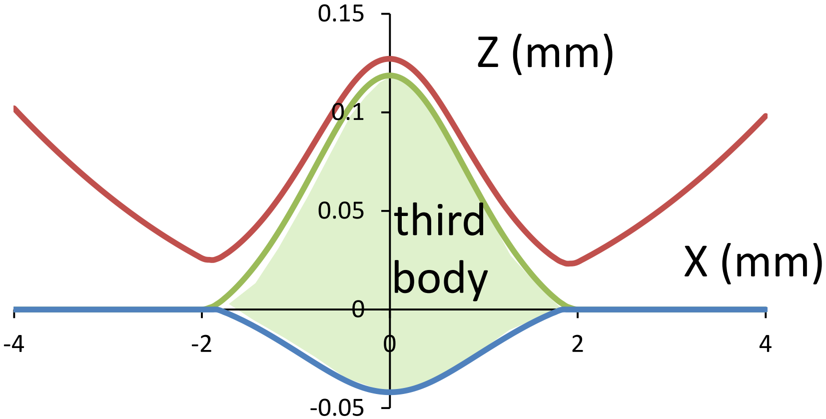

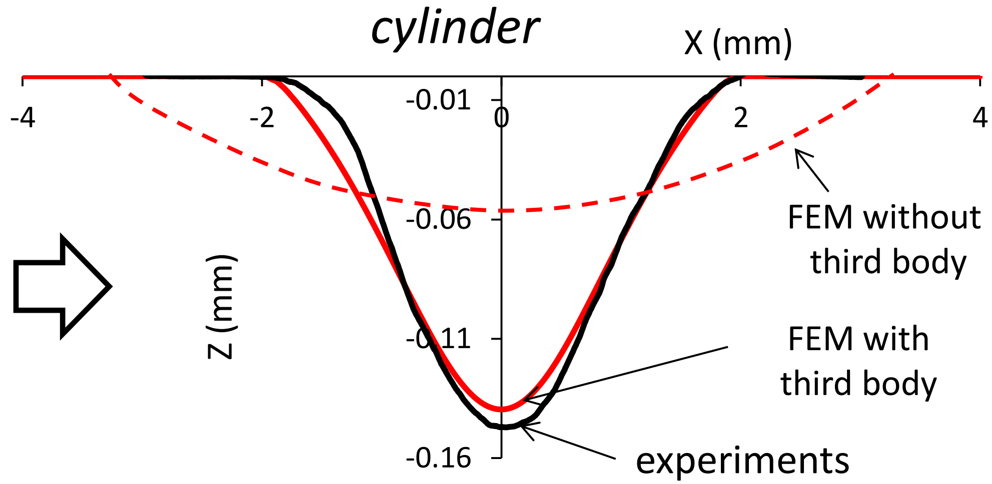

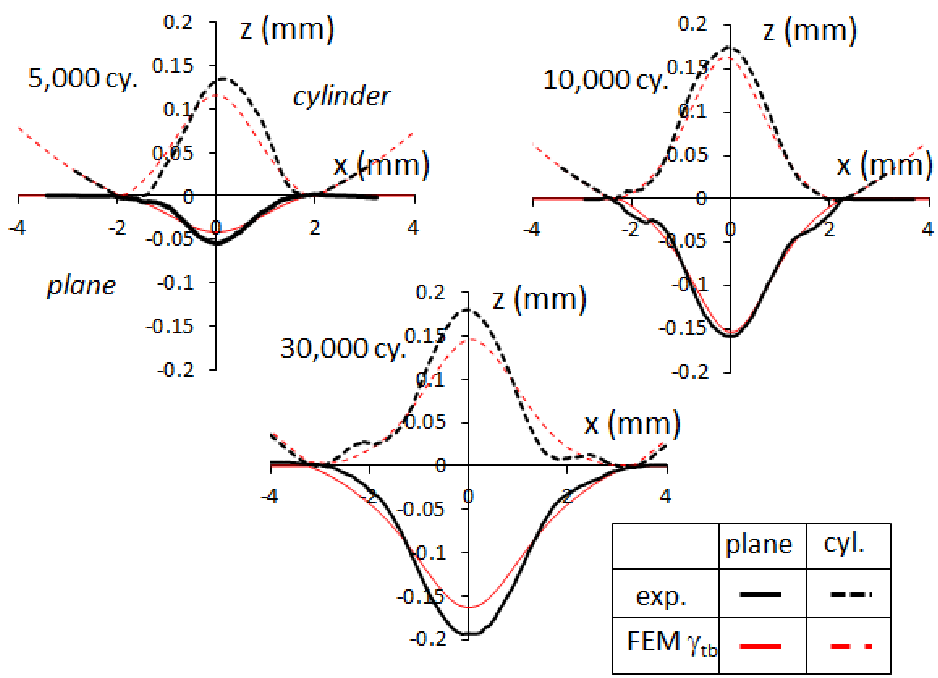

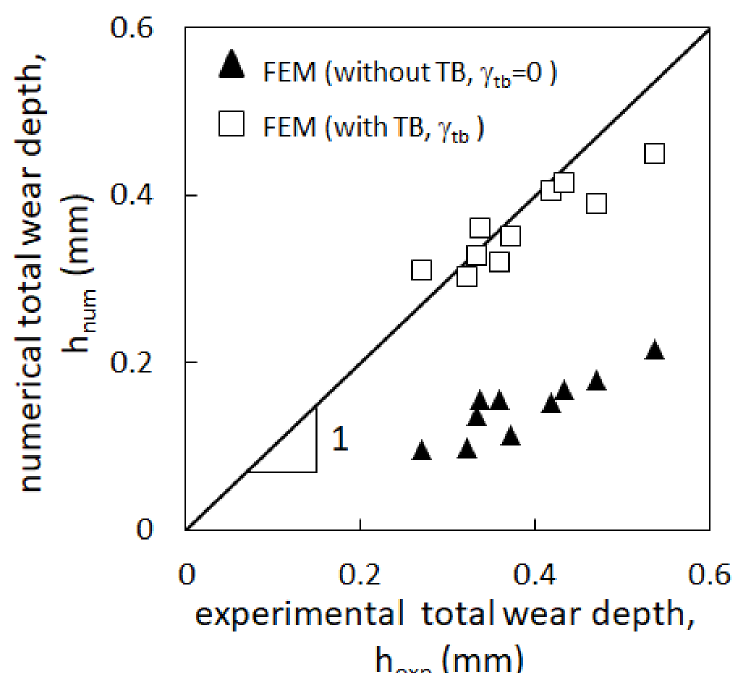

P. Arnaud, S. Fouvry, A dynamical FEA fretting wear modeling taking into account the evolution of debris layer, Wear, Volumes 412–413 (2018) 92-108

Fretting Cracking

blade / disk contacts in turbine engine

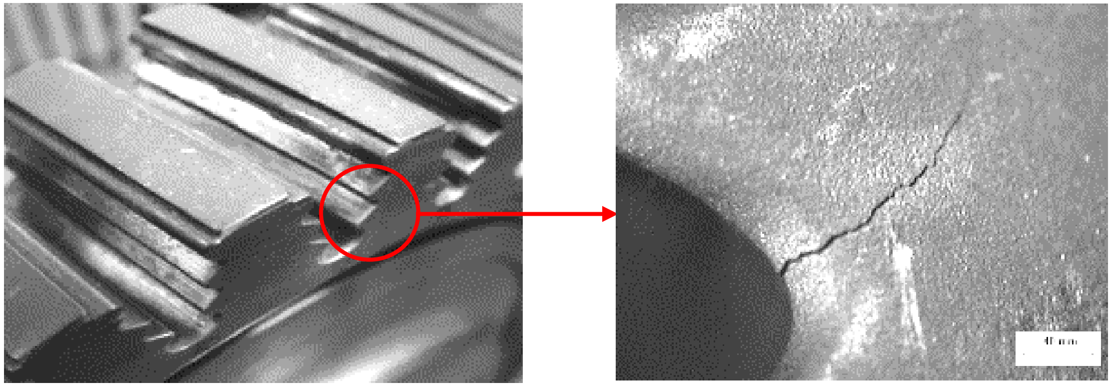

[M. Park et al.]

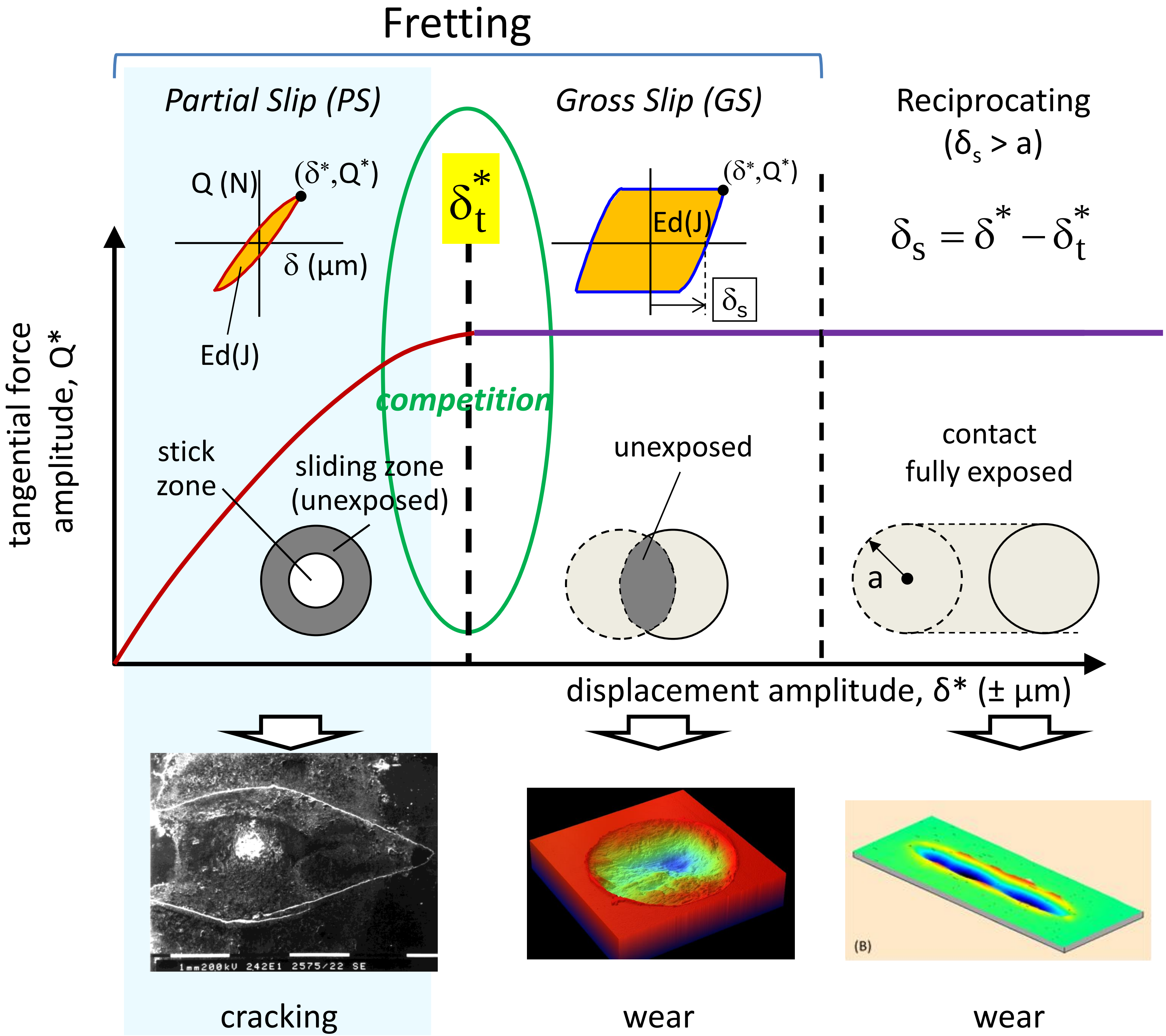

Fretting
Partial Slip (PS)
Gross Slip (GS)
Reciprocating
(δ_s > a)
Q (N)
(δ^*,Q*)
δ (µm)
Ed(J)
δ_t^*
Ed(J)
δ_s
$\delta_s = \delta^* - \delta_t^*$
tangential force amplitude, Q*
competition
stick zone
sliding zone (unexposed)
unexposed
contact fully exposed
a
displacement amplitude, δ* (± µm)
cracking
wear
wear
(B)

Industrial application : Pressed fitted Wheels-Axles contact

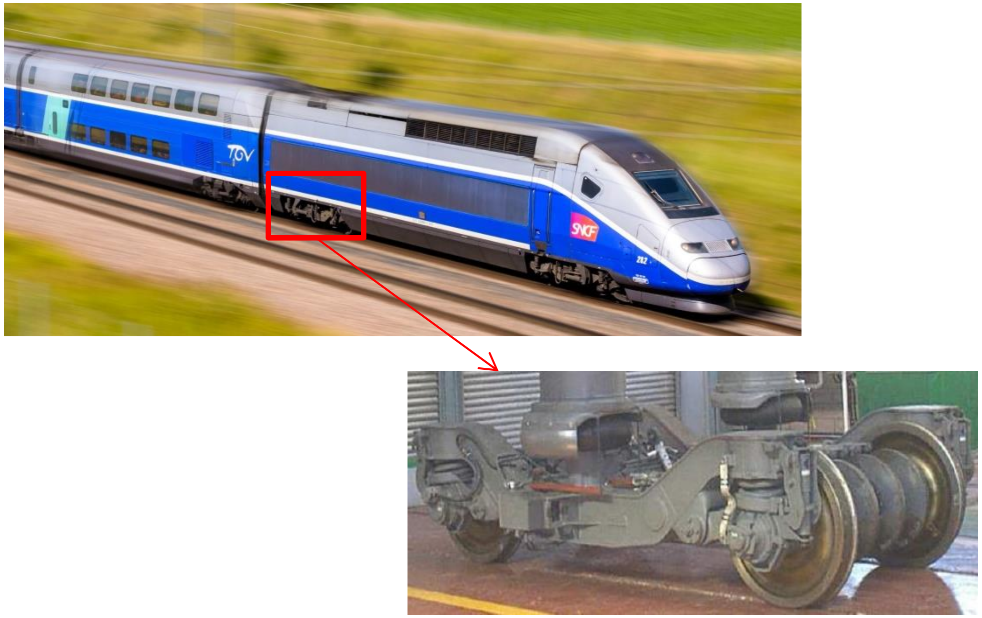

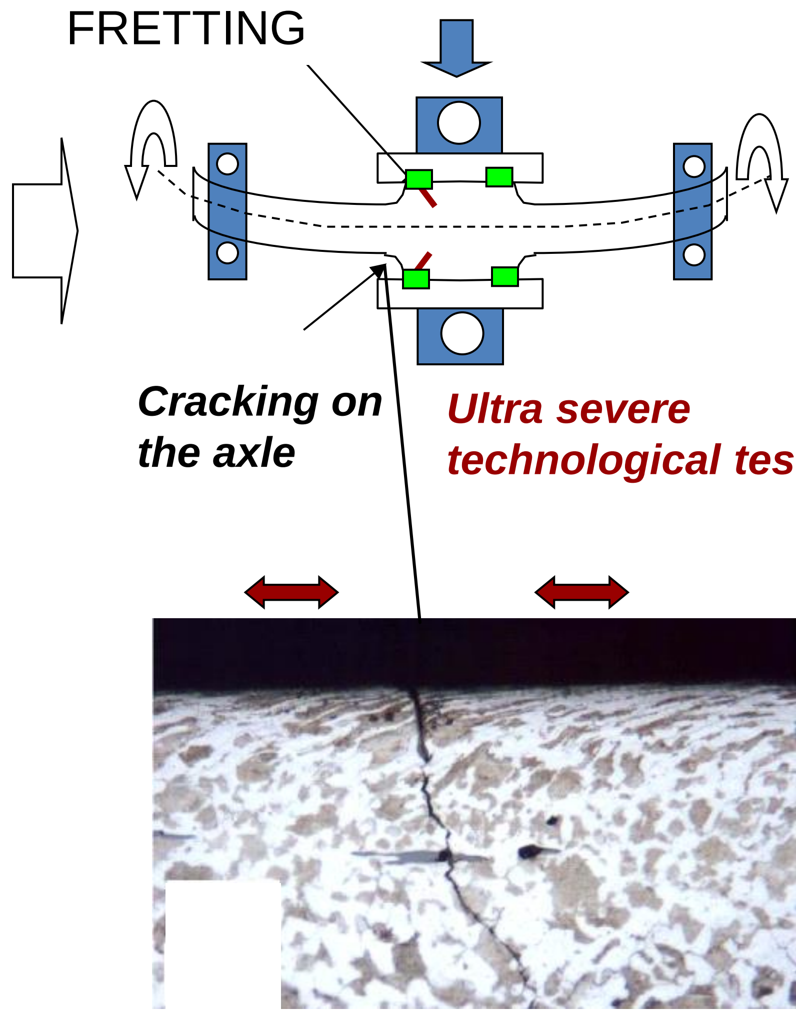

Fretting-Fatigue Loading

Fretting-Fatigue Loading ***(Partial Slip)***

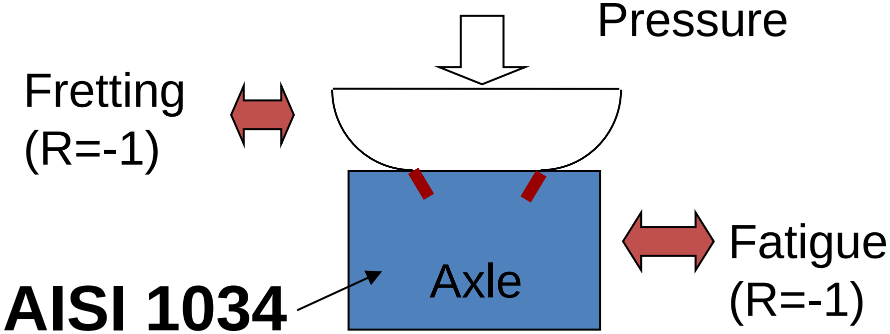

Question : Are can be predicted the cracking risk ?

Material : Low carbon steel (AISI 1034)

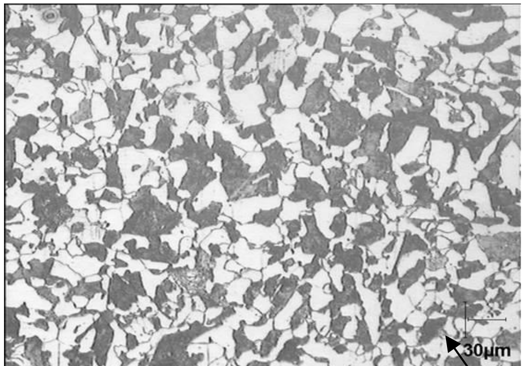

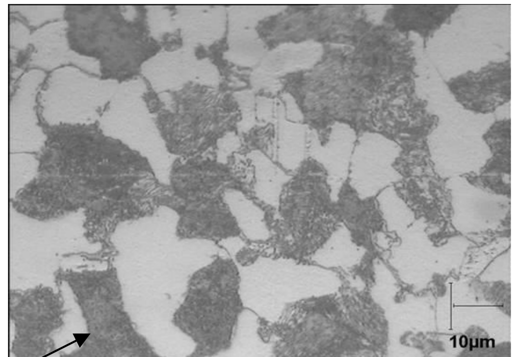

Ferrite - Perlite structure

Mechanical properties

Matériau	Low carbon steel
Young modulus, E (GPa)	200
Poisson coefficient, ν (ratio)	0.3
Yield stress, $Re_{0.2}$ (MPa)	350
Maximum stress, Rm (MPa)	600

Crack propagation (long crack) & fatigue

SIF range threshold, ΔK_0	7 $(MPa \cdot \sqrt{m})$
maximum SIF, K_c	117 $(MPa \cdot \sqrt{m})$
C coefficient (Paris law)	$2 \cdot 10^{-12}$
m exponant (Paris law)	3.5
Fatigue limite (R=1)	270 MPa

Gros V. , Ph.D Thesis, Ecole Centrale de Paris, France,1996.

Fretting Experiments : Coupling Between Plain Fretting & Fretting Fatigue tests

Plain Fretting Test (fretting wear test)

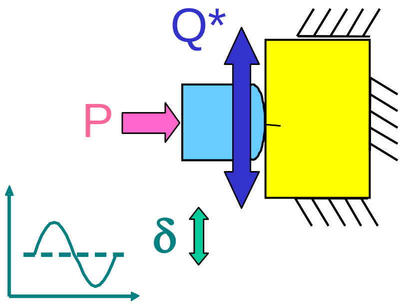

AISI 1034

52100

P= 230 N/mm
R= 40 mm
p_{0H}= 450 MPa , a_H = 320 µm

Fretting Fatigue Test

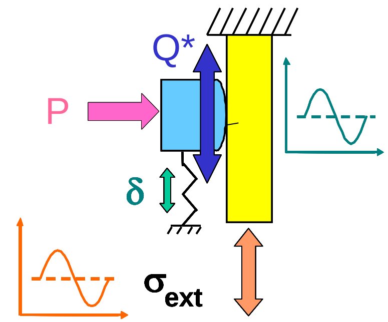

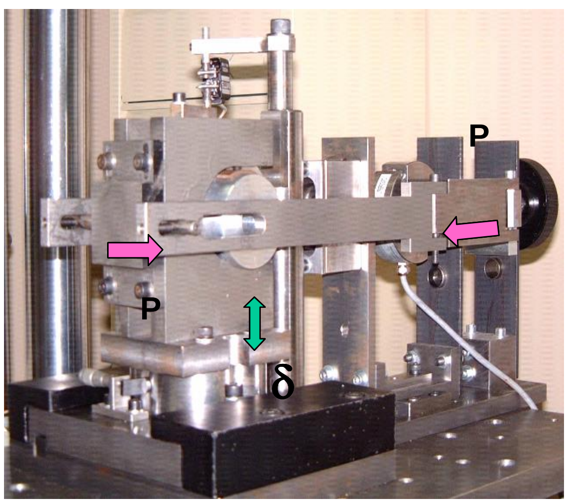

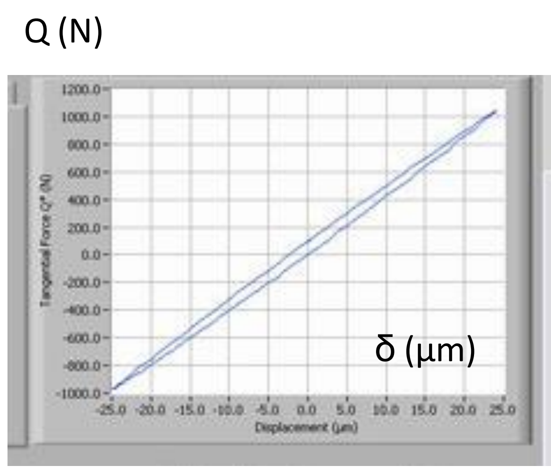

FRETING CYCLE
(Partial Slip)

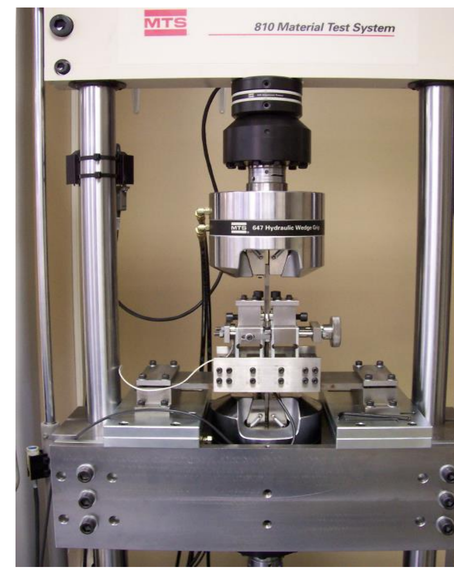

Fretting fatigue cracking

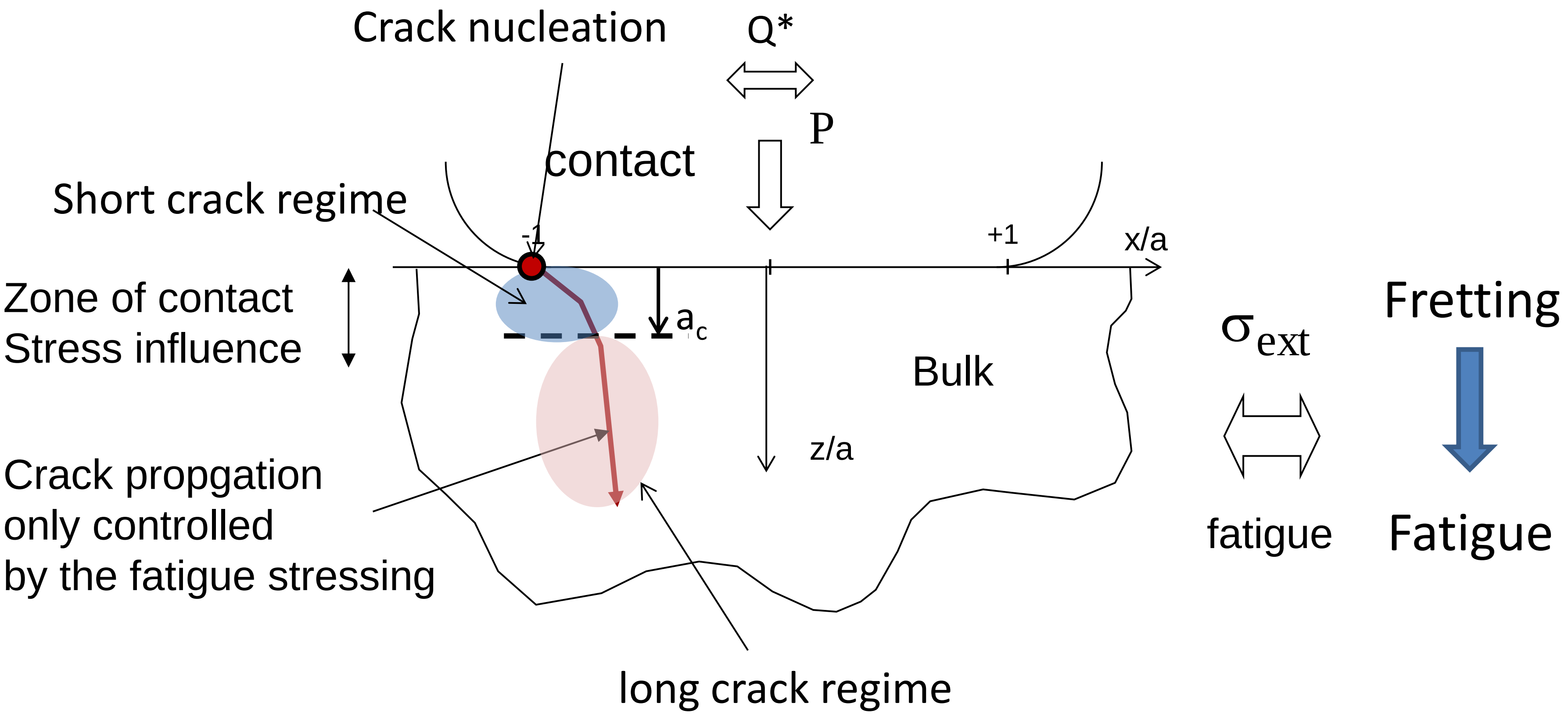

Fretting Fatigue : Stress & Damage evolutions

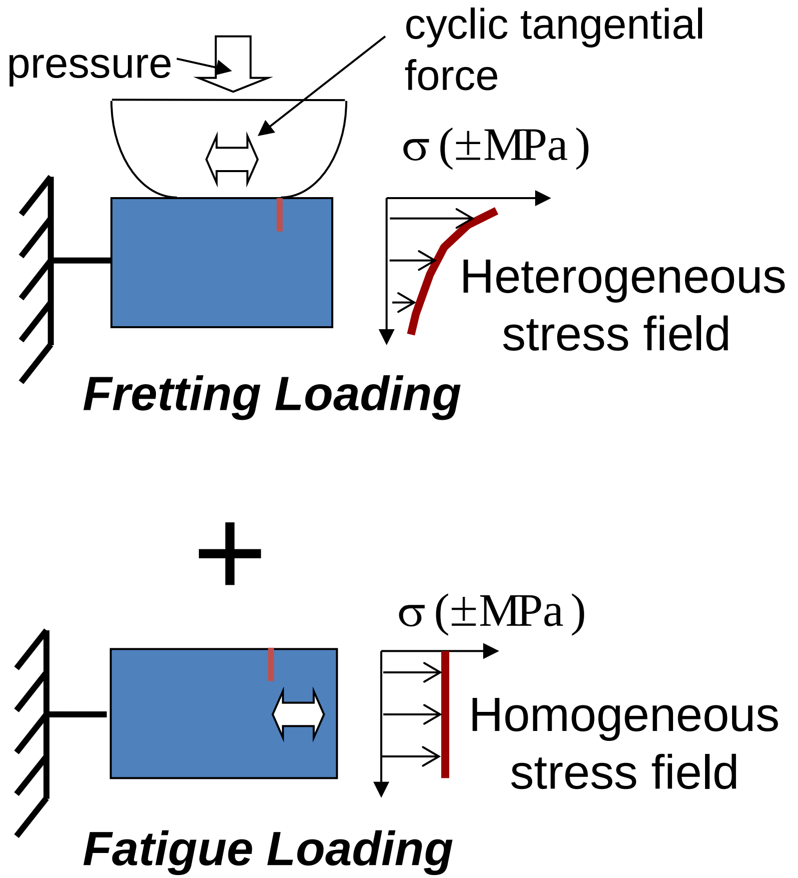

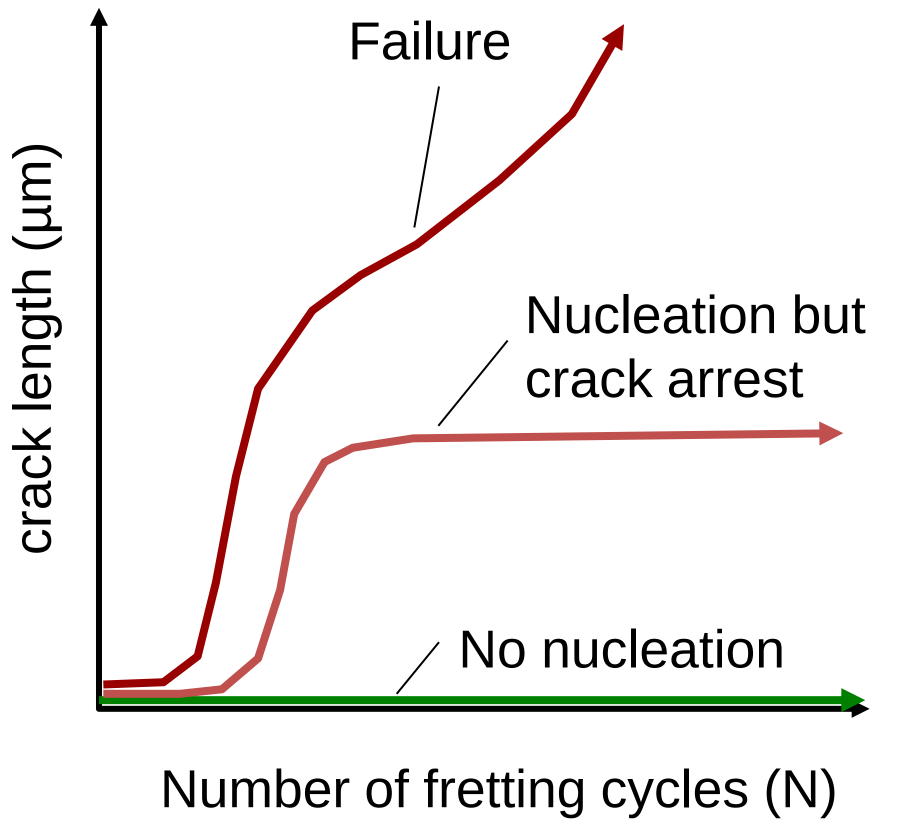

Fretting Fatigue : Fretting – Fatigue Map Concept (Partial Slip)

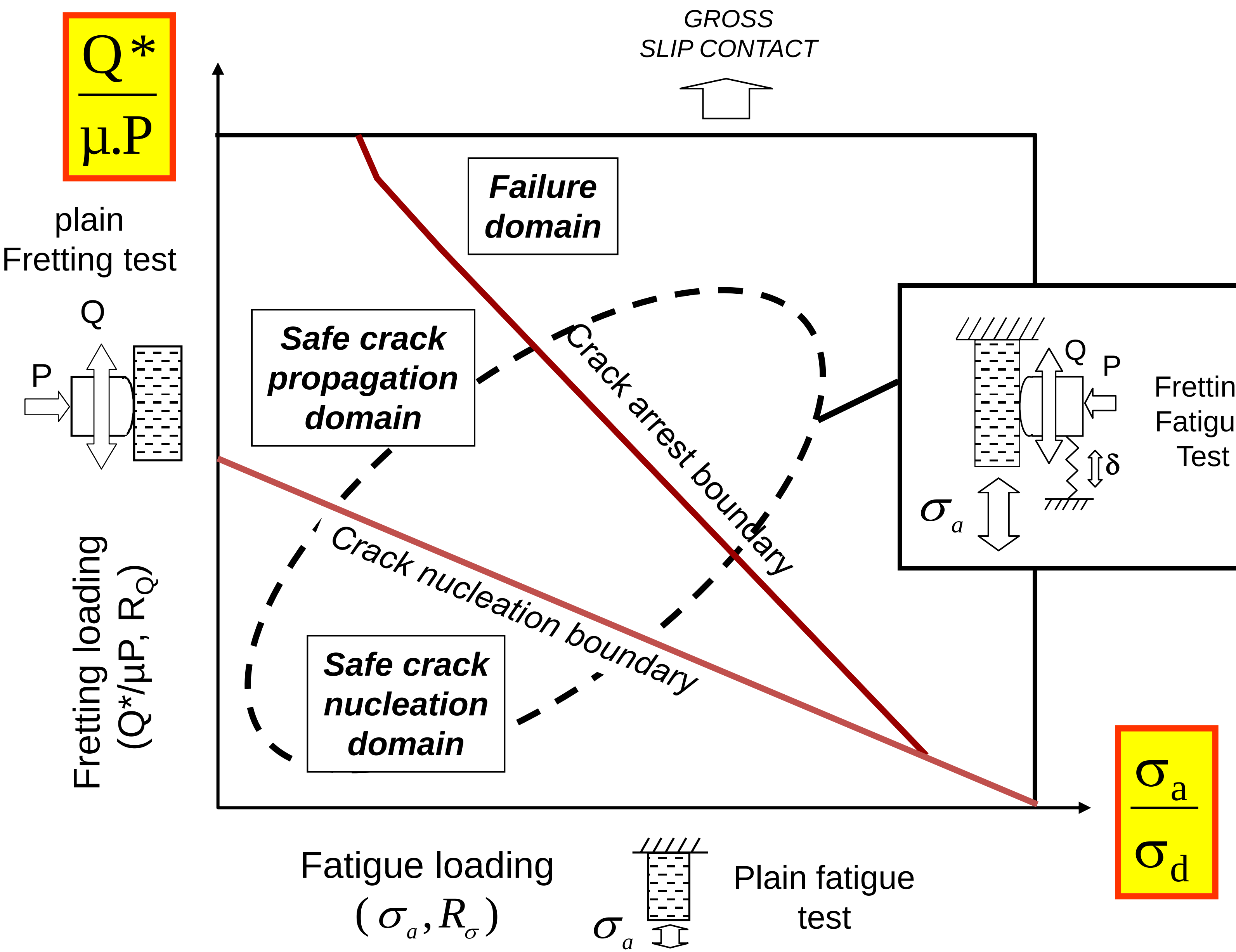

Fretting contact in the partial slip regime

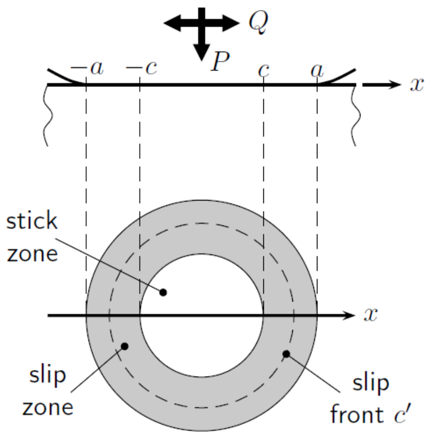

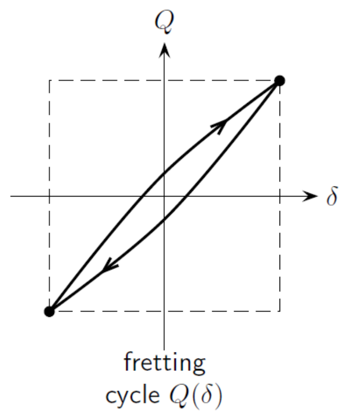

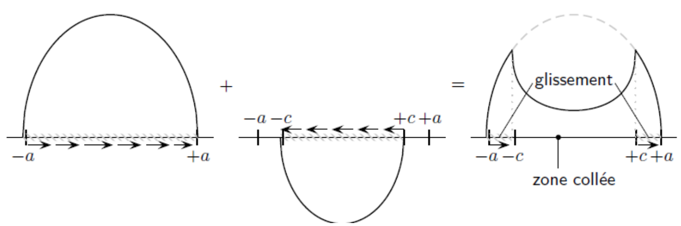

Evolution of the surface shear during the fretting cycle in partial slip predicted by the theory of Mindlin ($\mu = 0,5$ and $k = c/a = 0,5$) :

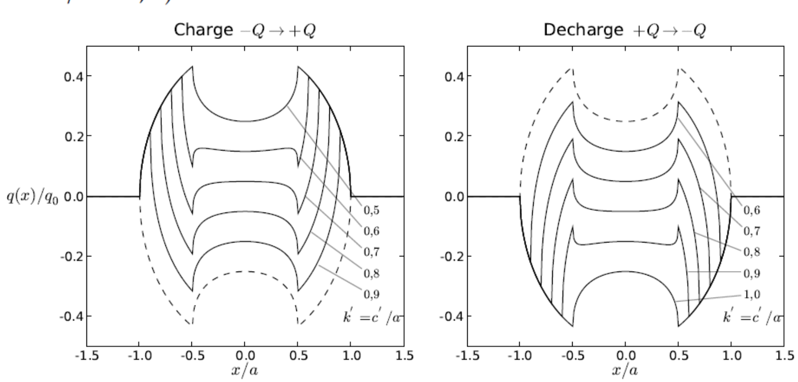

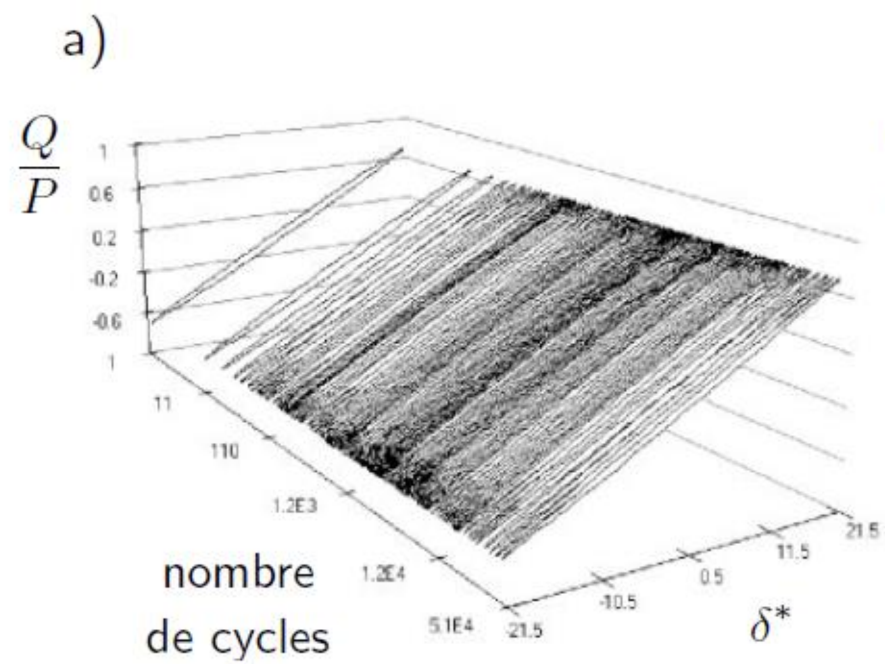

Analytical description of Plain Fretting and Fretting Fatigue contacts

Plain Fretting Contact

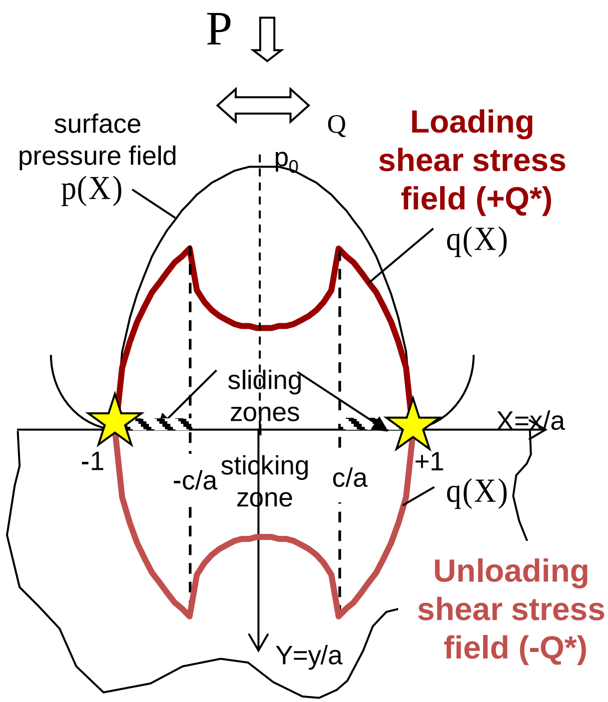

Mindlin et al, 1949

Fretting-Fatigue Contact

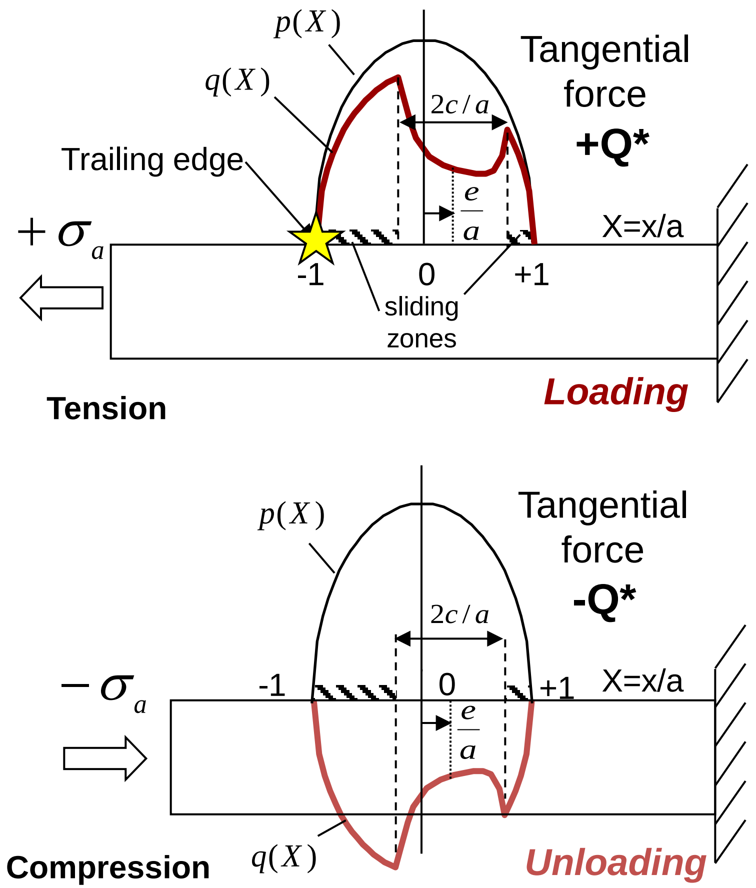

Nowell et al, 1989

Maximum loading located ☆ symetrically at the contact borders

Maximum loading located at the trailling edges (at the Loading state)

Contact modeling: Stress field analysis

FEM ANALYSIS

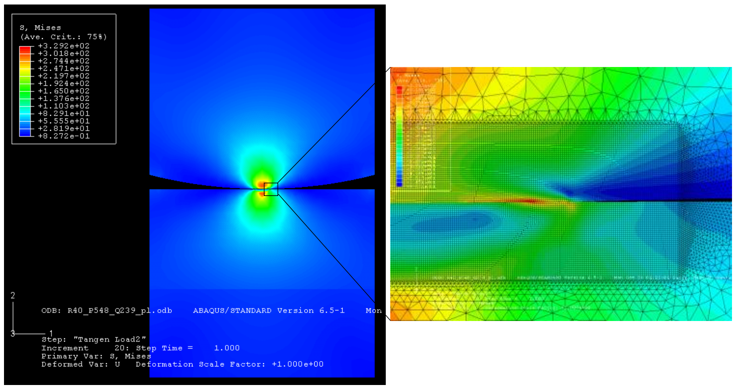

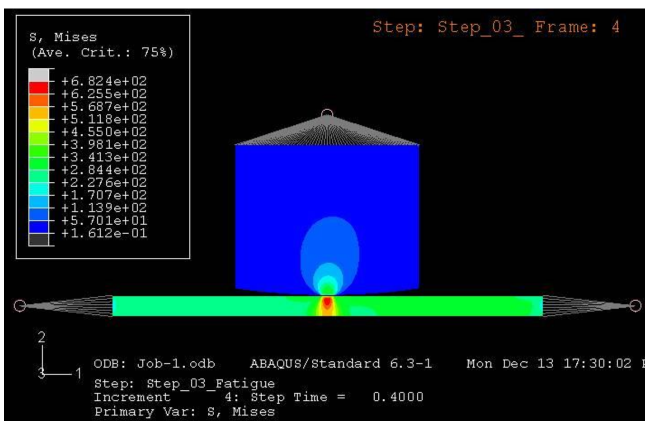

Poster, R. Amargier (Airbus)

Analytical formulation: Green's functions
Superposition of piecewise-line
Overlapping triangular elements
(K.L. Johnson, 1985)
[Elastic Half Space Hypothesis]

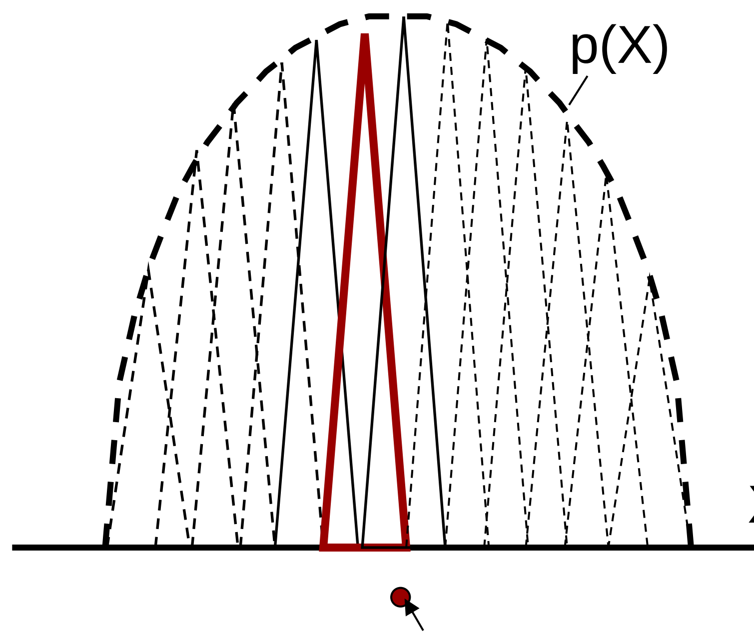

$$\Sigma(M, t) = \Sigma \Lambda$$

- Can include plasticity
- Long and fastidious (inappropriate to develop A mapping investigation !!)
- Very fast !!

Plain Fretting Wear Test → Friction Identification of the crack nucleation

Fretting Test : Q=± 200 N/mm, 10^6 cycles*

Surface observation

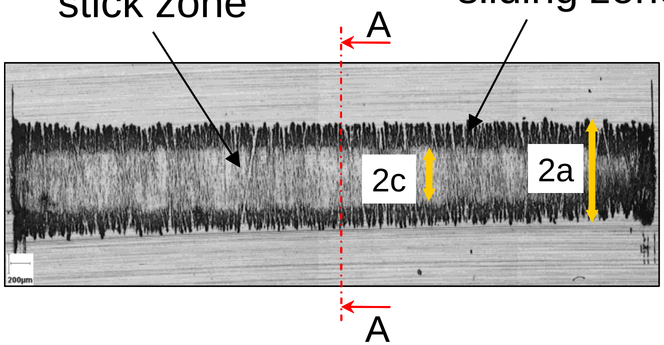

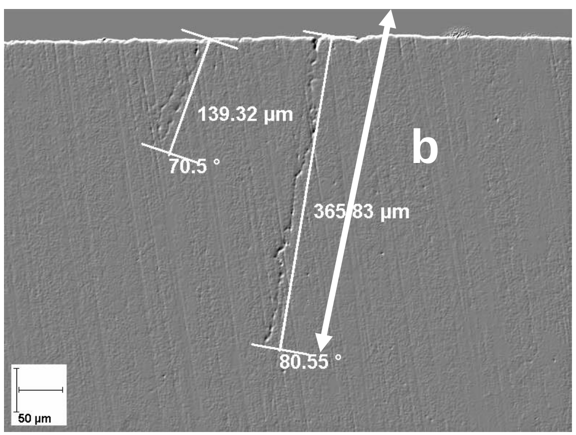

Cross section observation: measure of the crack length

10^6 cycles

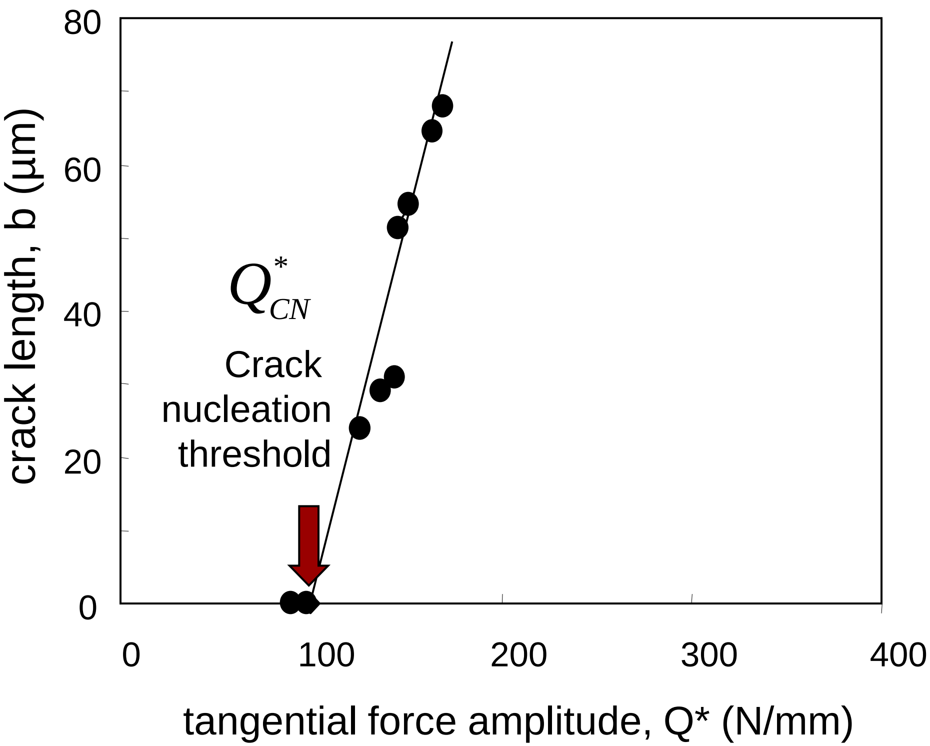

P=227N/mm, µ=0.85
(10^6 cycles, p_0= 450 MPa)

$$\Rightarrow \quad Q^*_{CN} = 100\,\mathrm{N/mm}$$

Plain Fretting

determination of the loading path

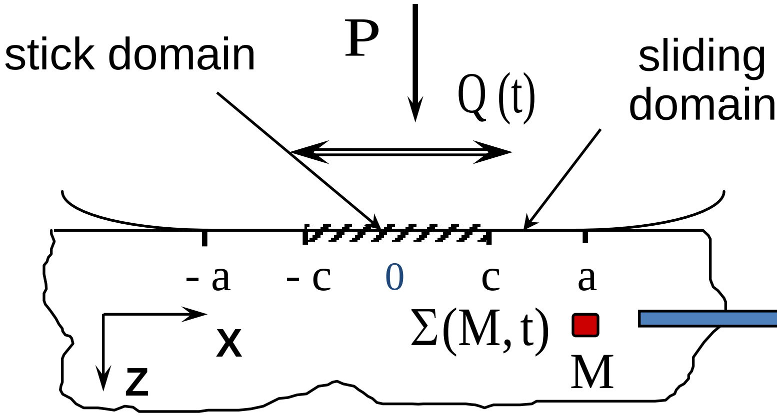

shakedown

point M fixed

$$\hat{\sigma}(t) = \rho^* + \Sigma(t)$$

computation of the cracking risk (Dang Van)

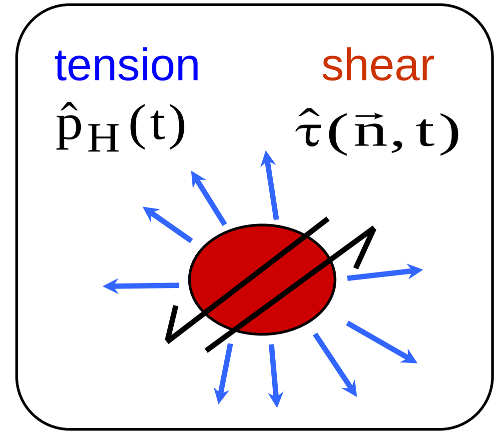

$$d_{DV} = \max_{t,\vec{n}} \left[\frac{\|\hat{\tau}(\vec{n},t)\|}{\tau_d - \alpha.\hat{p}(t)} \right]$$

if $d_{DV}>1$ cracking

$$\alpha = \left(\tau_d - \sigma_d/2\right) / \left(\sigma_d/3\right)$$

$$\alpha_C = \frac{\tau_d - \sigma_d/\sqrt{3}}{\sigma_d/3}$$

σ_d : alternating bending fatigue limit

τ_d : alternating shear fatigue limit.

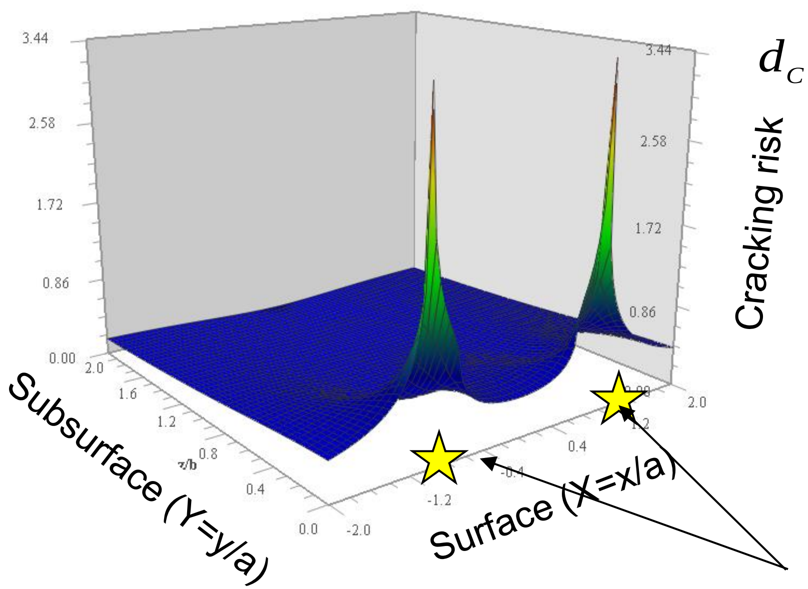

Cracking at the contact borders

Application of the Dang Van (Quantitative Prediction)

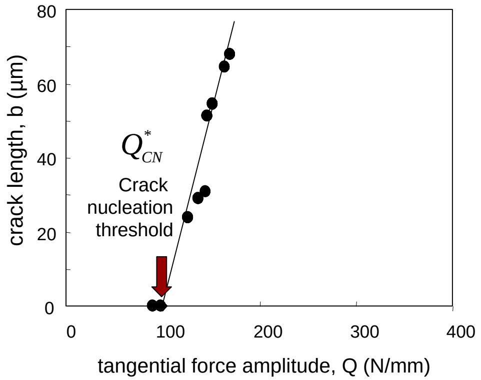

P=227N/mm, µ=0.85

(10^6 cycles, p_0= 450 MPa)

$$Q^*_{CN} = 100\,N/mm$$

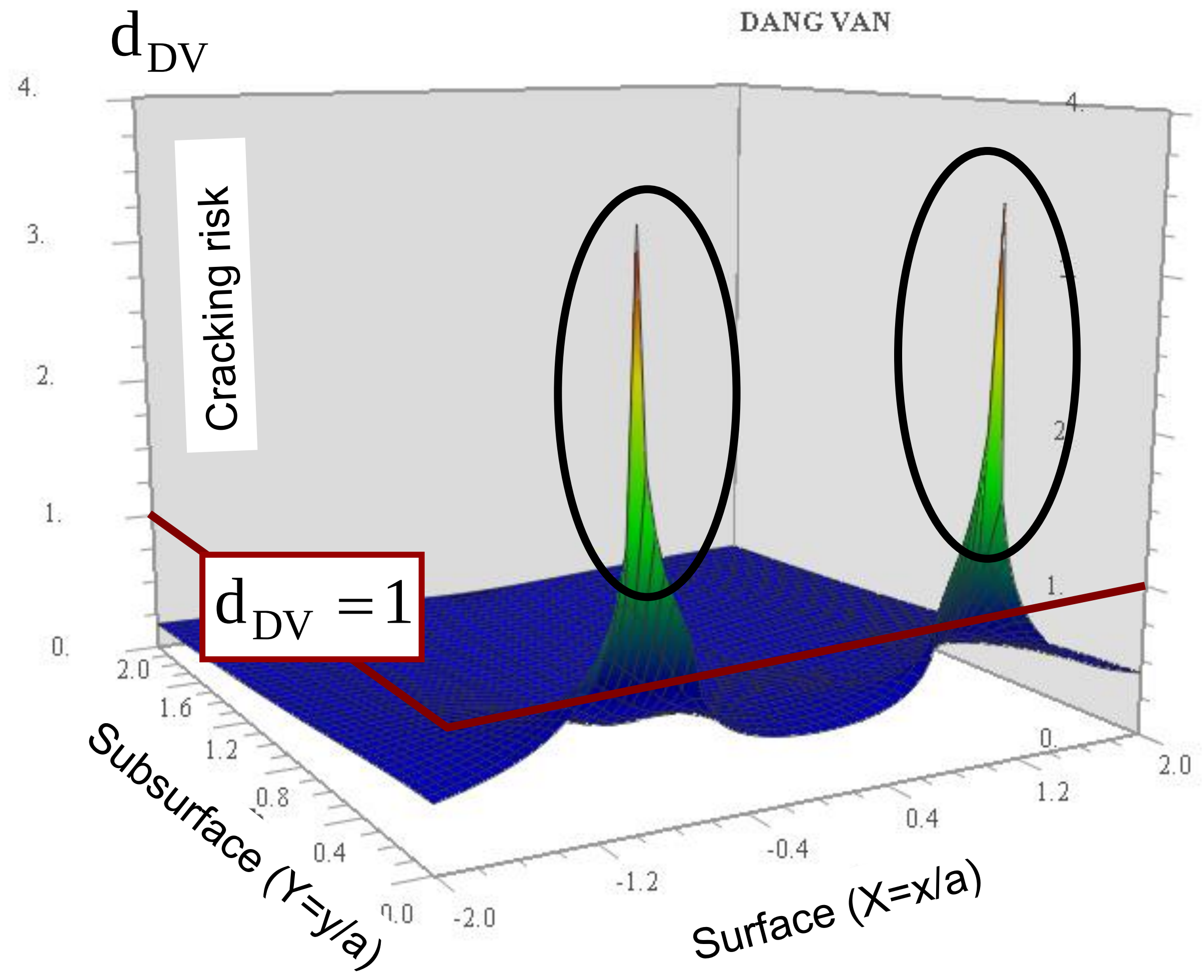

➡ Overestimation of the cracking risk !!

"Non local approach" to capture stress gradient effects

General 3D stress state condition

nucleation process volume approach

Critical distance method

2D plane strain condition (cylinder/plane)

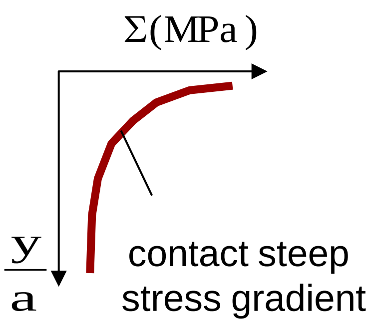

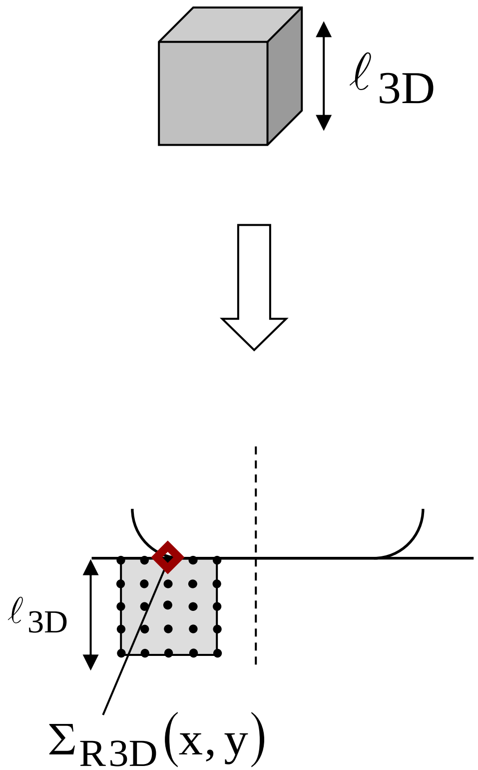

Averaging over a square surface

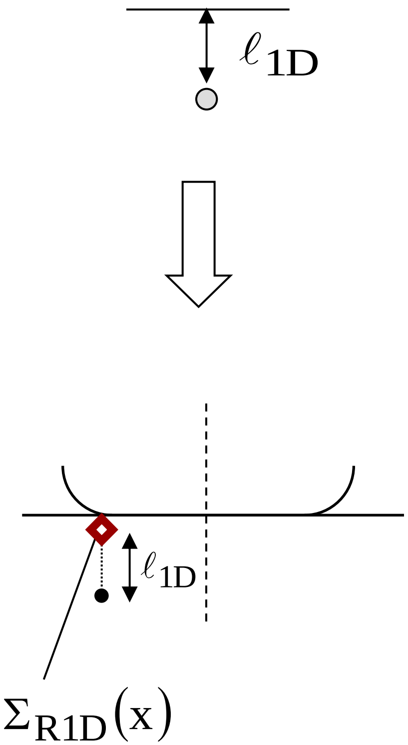

Stress analysis At a critical distance of the stress discontinuity

Identification of representative length scales (Dang Van)

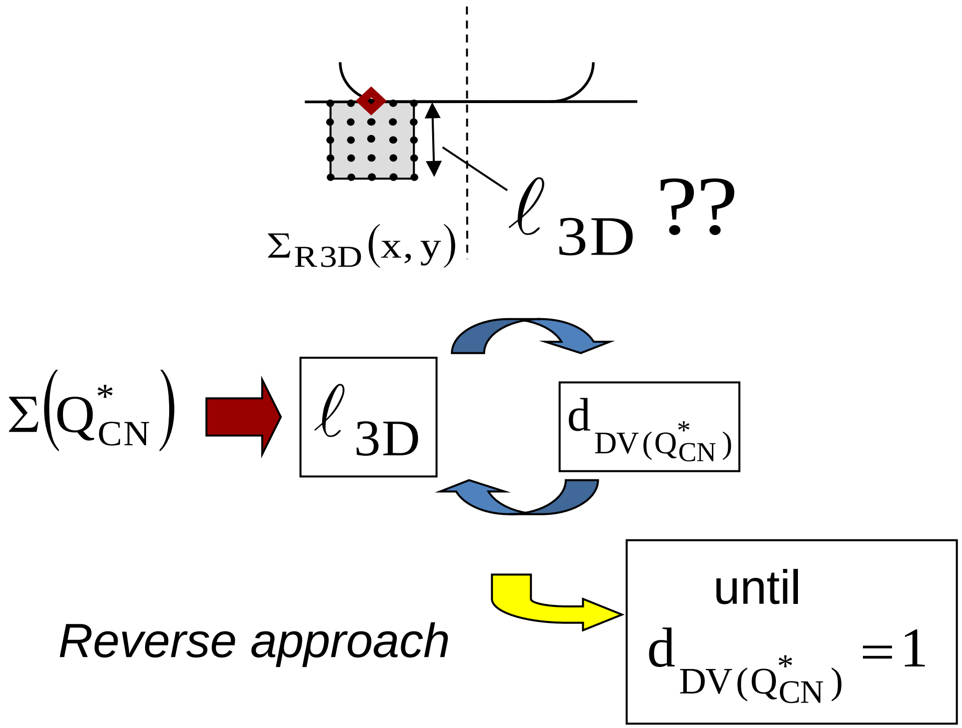

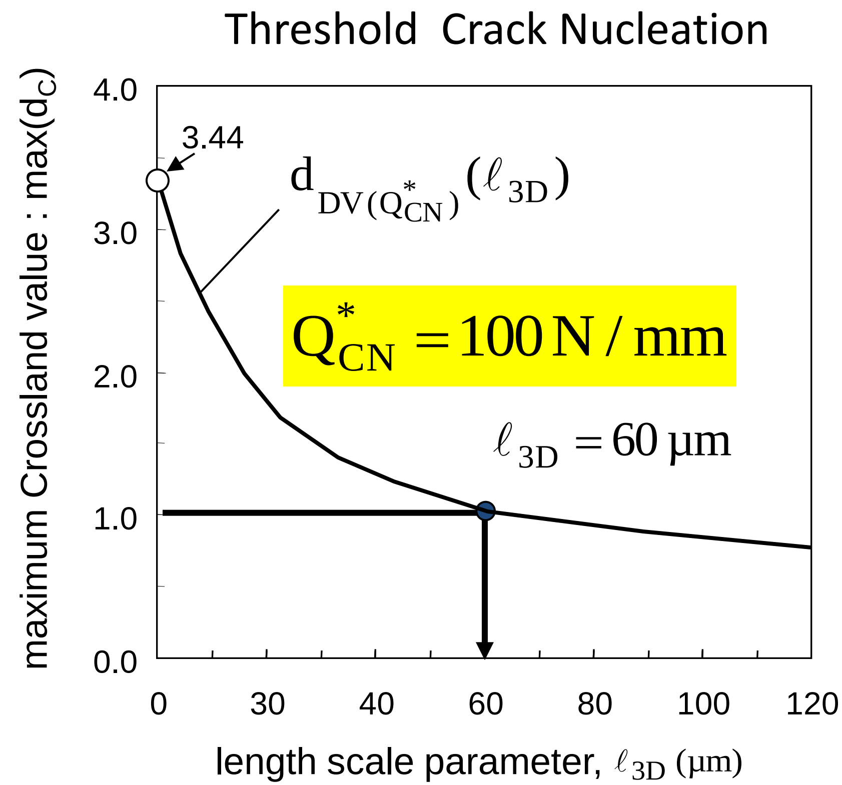

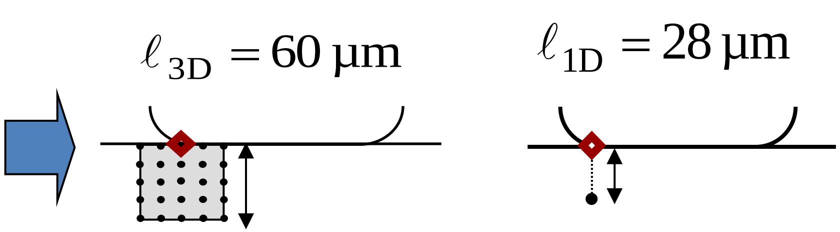

$$\ell_{3D} \approx \ell_{2D} \approx \frac{\ell_{1D}}{2}$$

Consistent with notch description (Taylor and al)

Fretting – Fatigue Experiments : Identification of the crack nucleation Fretting Fatigue map

Fatigue stress amplitude : σ_a [MPa] (R=-1)	Tangential force amplitude Q* [N/mm] (R=-1)	Cross section Examination 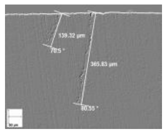
50	92	CRACK
50	82	NO CRACK
100	115	CRACK
100	110	CRACK
100	100	CRACK
100	80	NO CRACK
100	62	NO CRACK
120	91	CRACK
120	78	NO CRACK

10^6 cycles

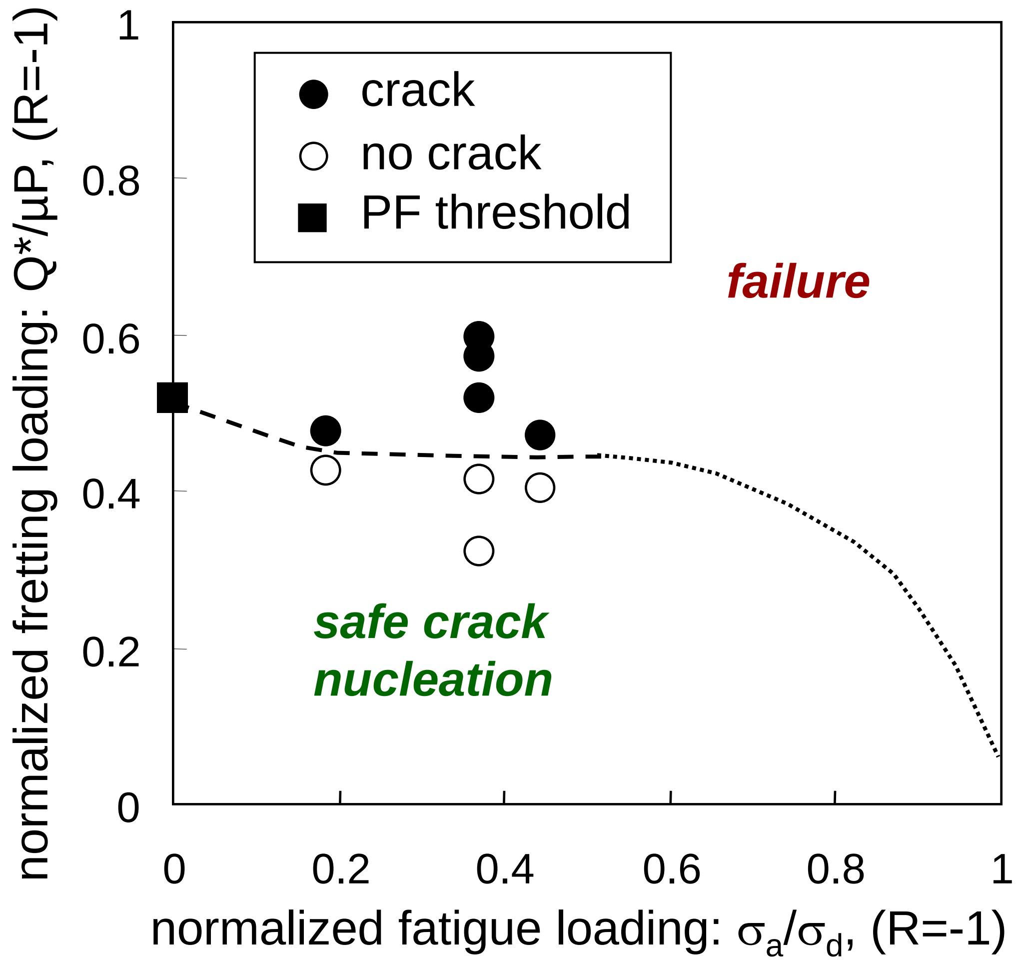

Low influence of fatigue stress amplitude in the low fatigue stress range !
(Conventional idea : crack nucleation is controlled by fretting)

Correlation Experiments // Modelling

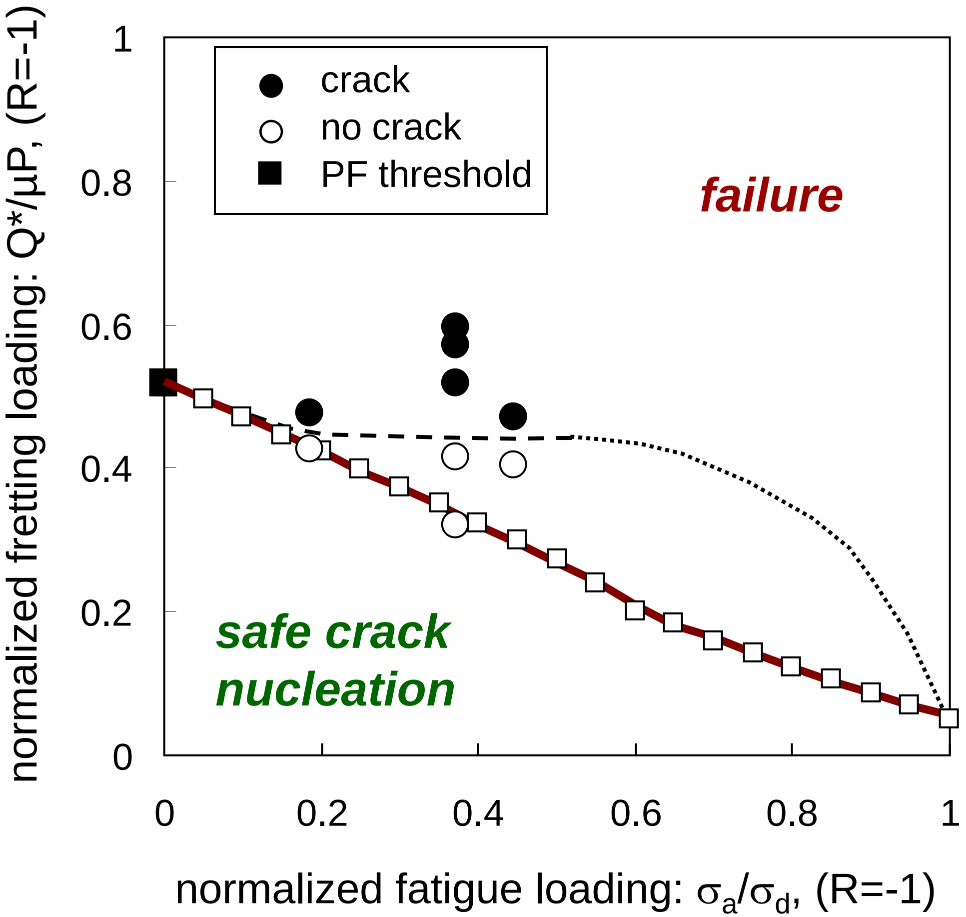

Theoretical prediction of the Fretting Fatigue crack nucleation boundary

$d_{DV} = 1$

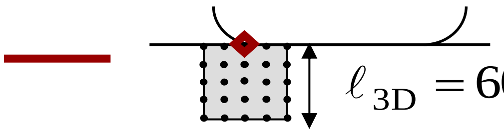

$\ell_{3D} = 60\ \mu m$

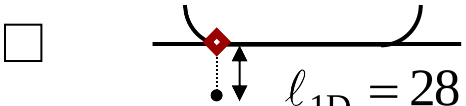

$\ell_{1D} = 28\ \mu m$

Similar tendencies !!

Pessimistic (i.e. secure) prediction of the safe crack nucleation domain from Plain Fretting identification !

How to prediction the Crack Arrest ?

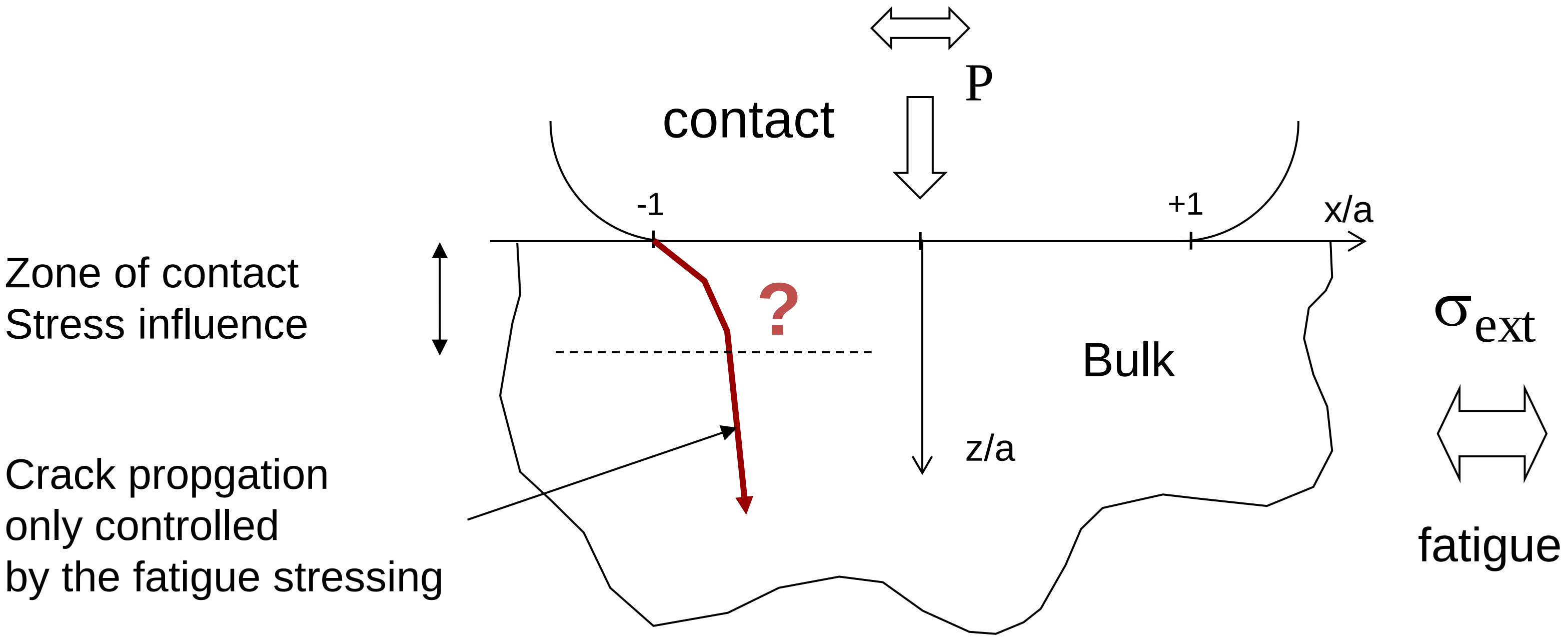

FEM modelling

FEM code (ABAQUS):

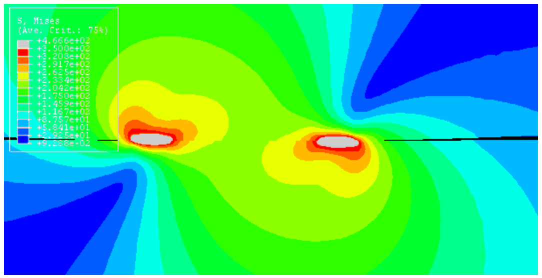

Identification des zones de glissement

Insertion of the crack (Crack Box)

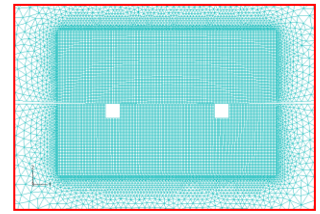

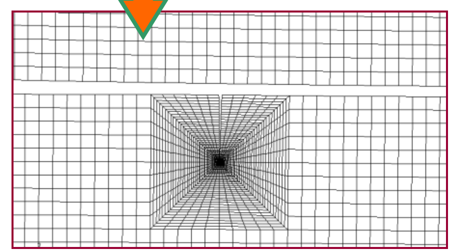

- CPE4
- mesh = 20 µm
- refine meshing at the crack tip

Z-Crack

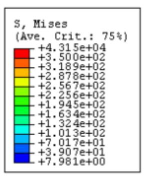

Sens du déplacement

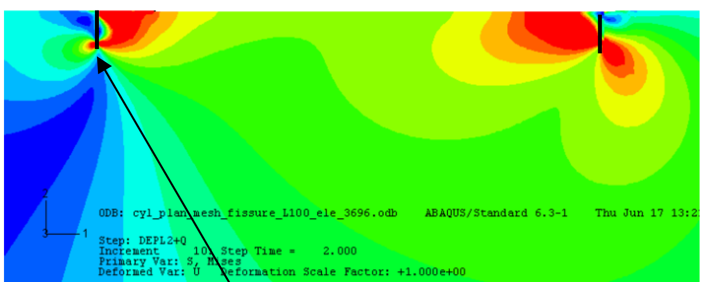

Computation of SIF K_I, K_{II} & K_{III}

J integral (Eshelby, Rice)

$$G = J = \frac{K_1^{\ 2}}{E'} + \frac{K_2^{\ 2}}{E'} + \frac{K_3^{\ 2}}{2\lambda}$$

Evolution of the SIF below the contact: Non monotonic evolution !

Increase of the crack length

Decrease of the contact Stress field

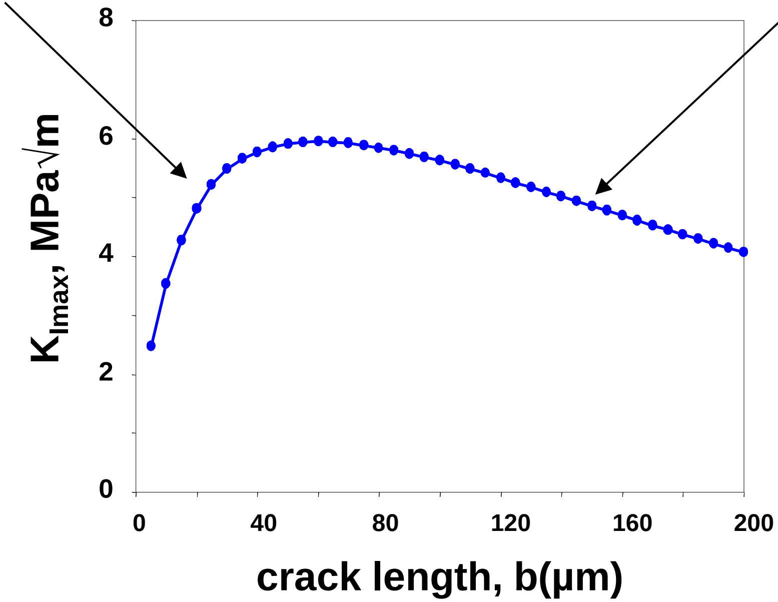

Plain Fretting

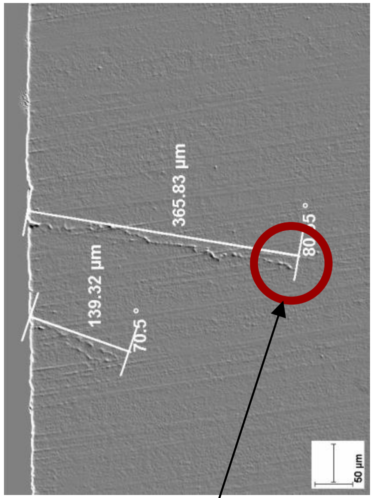

Plain Fretting condition

Q*= 125 N/mm
P= 230 N/mm

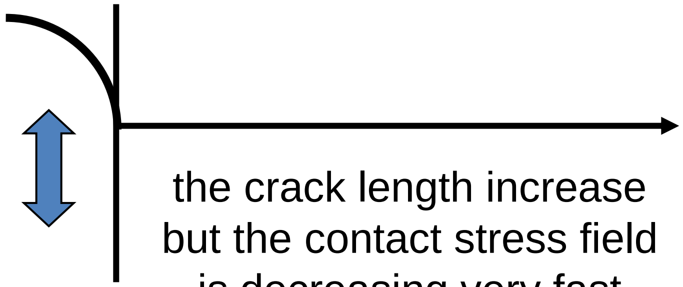

The crack stops !

The crack stops ! (situation of plain fretting condition)

Determination of the effective SIF (combining mode I and II)

General formulation $\Delta K_{eff} = \sqrt{\Delta K_{Ieff}^{\ 2} + \Delta K_{IIeff}^{\ 2}}$

- Pure mode I (Usual hypothesis)

$$\Delta K_{eff\_I} = K_{Imax}$$

Because R=-1 (closure effect)

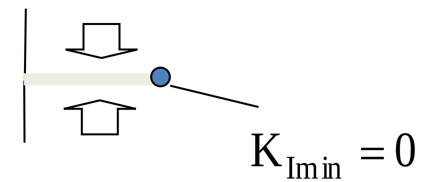

- Mixed Mode B (Crack edge friction free)

$$\Delta K_{eff\_mixed\ (\mu c=0)} = \sqrt{K_{Imax}^{\ 2} + (K_{IImax} - K_{IImin})^2}$$

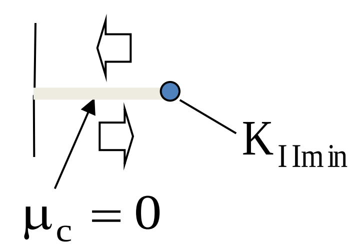

$$\Delta K_{eff\_I} < \Delta K_{eff\_mixed\ (\mu c=0)}$$

Paris Erdogan diagram

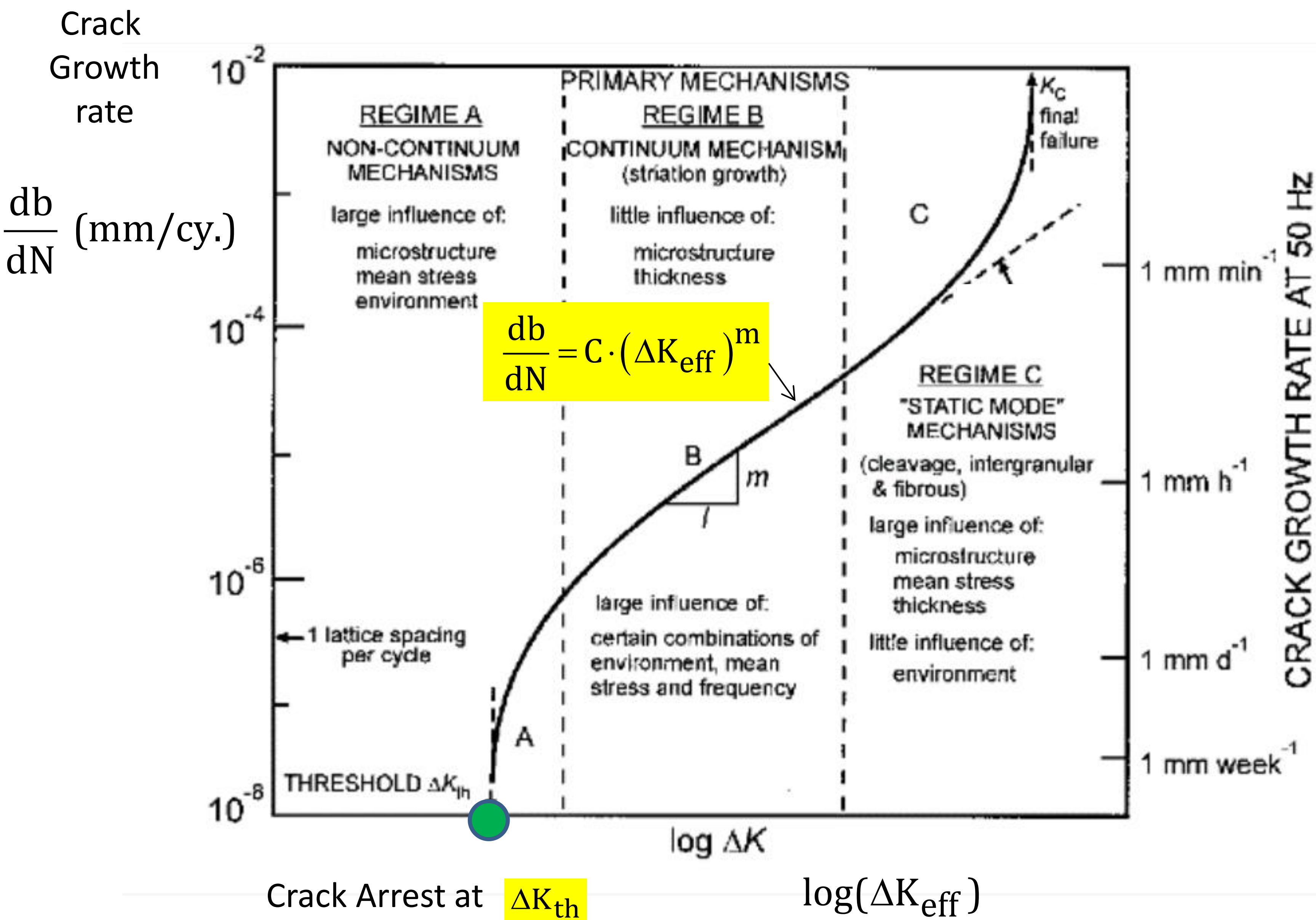

Alternative crack arrest approach : El Haddad et al. formulation

Specific behavior of the crack arrest condition for the small crack !!!

El Haddad approach

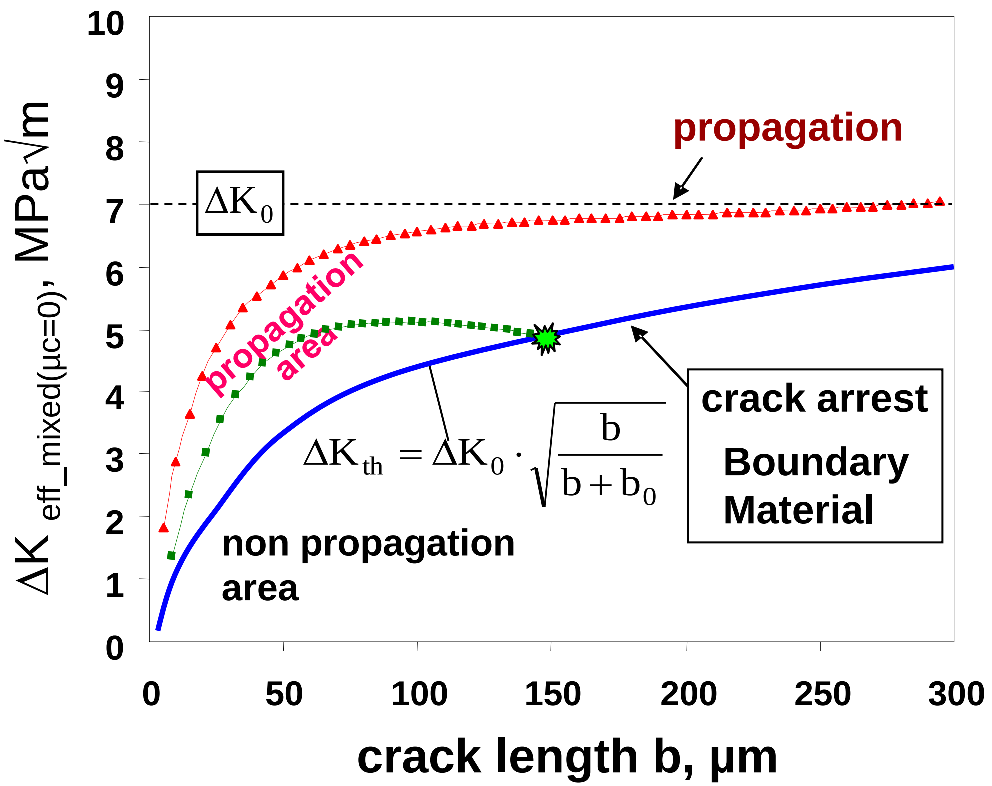

Crack arrest approach based on the El Haddad et al approach

Crack Boundary

$$\Delta K_{th} = \Delta K_0 \cdot \sqrt{\frac{b}{b+b_0}}$$

$$b_0 = \frac{1}{\pi}\left(\frac{\Delta K_0}{\sigma_f \cdot H}\right)^2$$

b_0 = 170µm

Long crack threshold, ΔK_0 = 7 MPa√m

Fatigue limit : $\sigma_f = 270$ MPa

Continuous evolution of the crack arrest boundary (more conservative)

Fretting – Fatigue Experiments : Identification of the crack arrest Fretting Fatigue map

10^7 cycles

Fretting Fatigue Test (10^7 cycles)	Fatigue stress amplitude : σ_a [MPa] (R=-1)	Tangential force amplitude Q* [N/mm] (R=-1)	Maximum crack length expertised : b (µm)
FF10	120	145	344
FF11	120	125	290
FF12	120	100	59
FF13	130	145	broken
FF14	130	125	broken
FF15	130	100	broken
FF16	140	125	broken
FF17	150	125	broken
FF18	160	125	broken

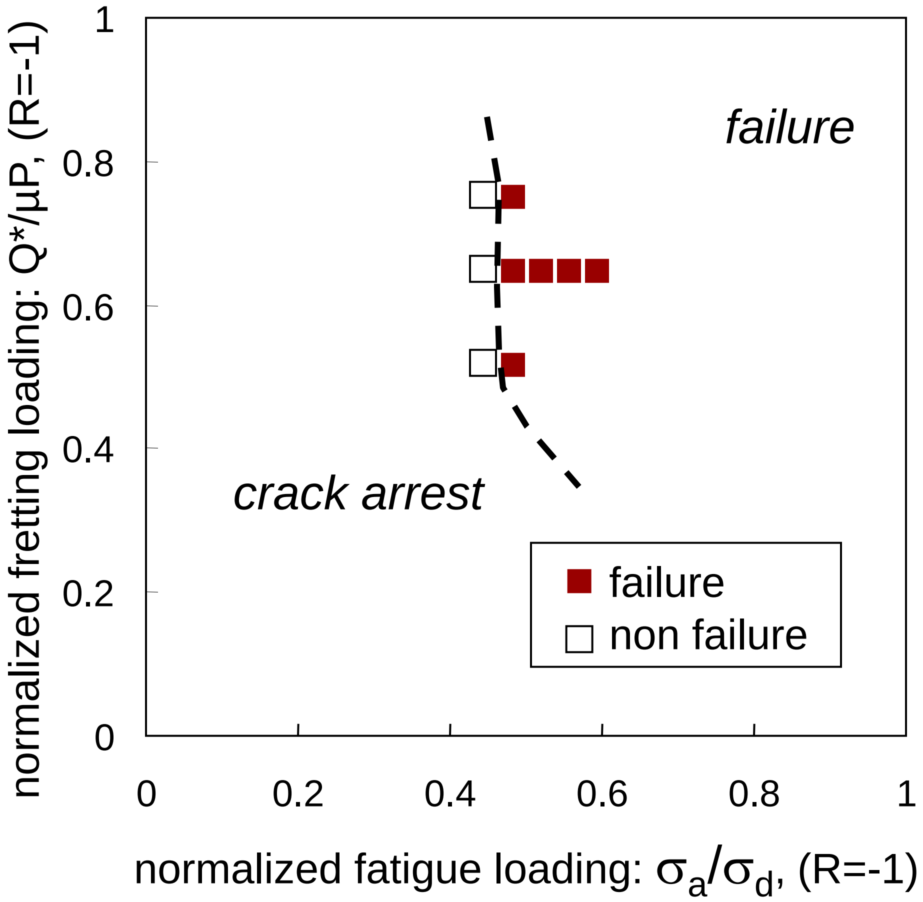

Low influence of fretting stressing on the crack arrest boundary !
(Conventional idea : crack propagation is controlled by fatigue)

CAFFM: Comparison between experiments & Modelling (EH et al. hypothesis of Crack arrest process)

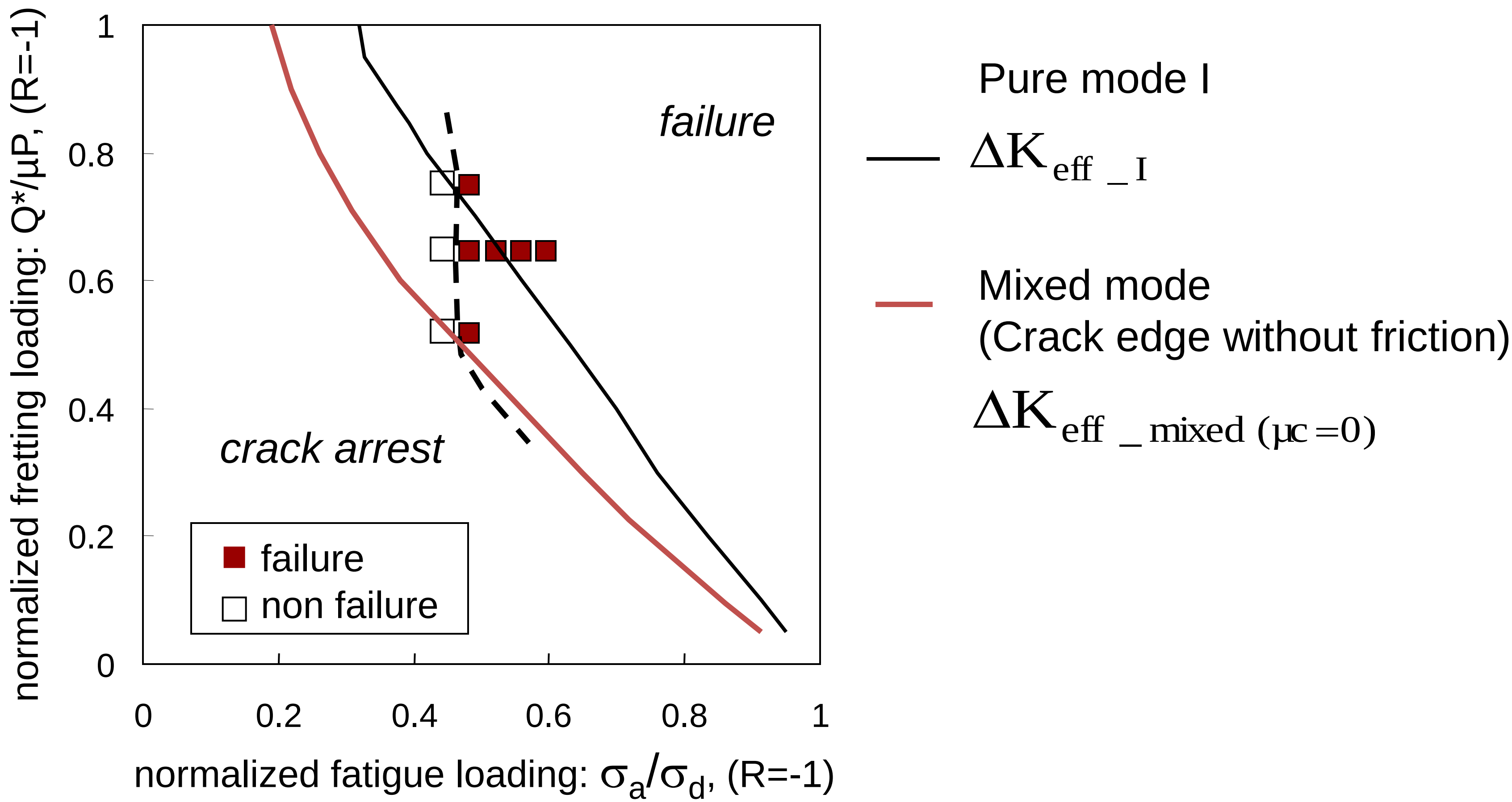

Mixed mode (Crack edge without friction) $\Delta K_{eff\_mixed\ (\mu c=0)}$ + El Haddad's Short crack Arrest → Most representative & conservative prediction of the Crack arrest boundary

FFM: Synthetic Fretting Fatigue Map

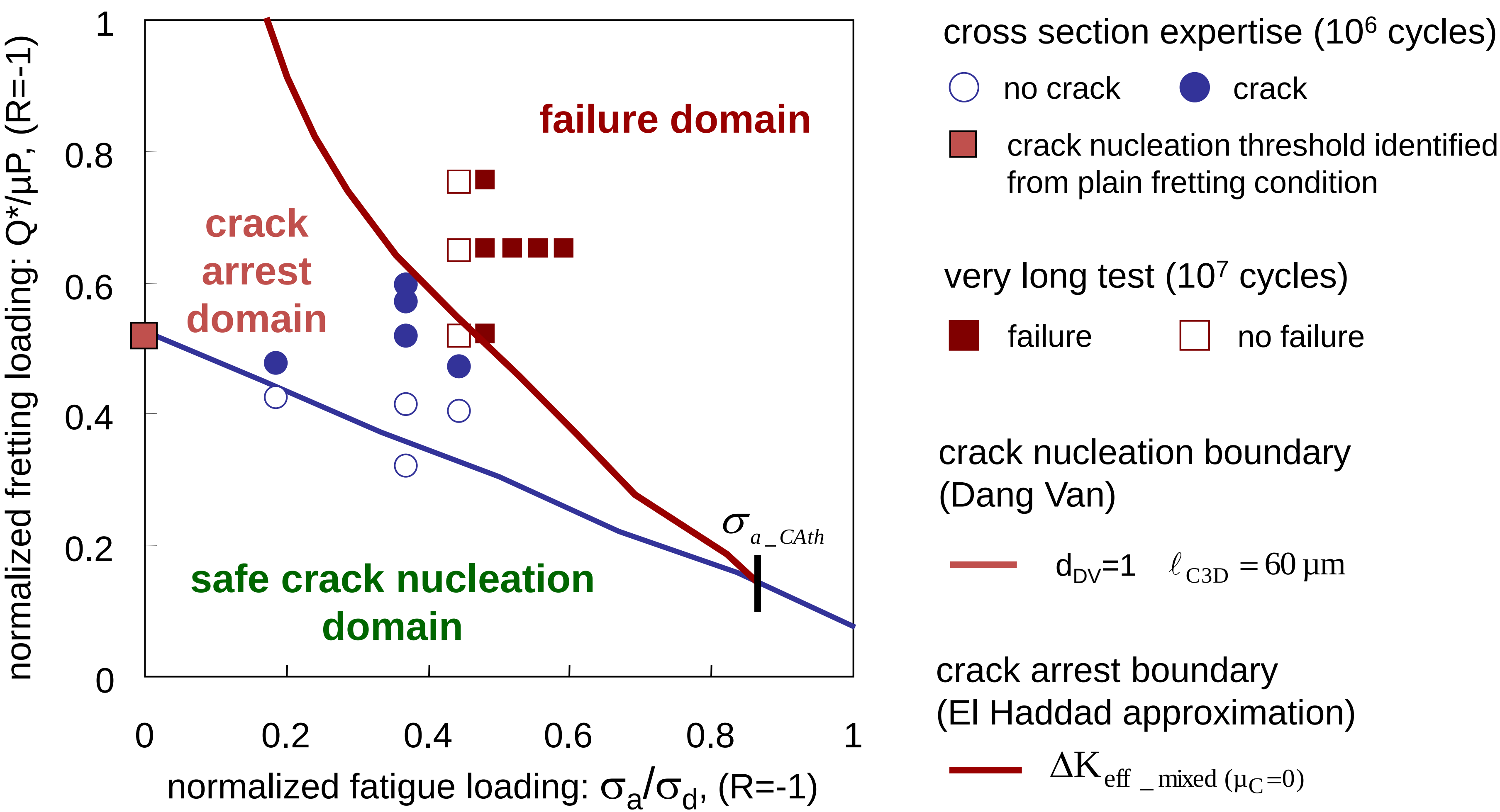

Conclusions

- A Fretting-Fatigue Mapping is introduced to formalize the cracking damages (Relative impacts of contact fretting & fatigue loadings are quantified)

- The crack nucleation boundary can be predicted combining a Multiaxial fatigue approach (Crossland) but taking into account stress gradient effects (Length scale identification from plain fretting test is validated : safe prediction of the crack nucleation boundary)

- The crack arrest boundary can be predicted combining mixed mode crack edge friction free estimation of the effective SIF range and a El Haddad description of the short crack arrest description.

S. Fouvry, K. Kubiak, Introduction of a fretting-fatigue mapping concept: Development of a dual crack nucleation – crack propagation approach to formalize fretting-fatigue damage, International Journal of Fatigue (2009), 31, 250-262.

R. Amargier, S. Fouvry, L. Chambon, C. Schwob, C. Poupon, Stress gradient effect on crack initiation in fretting using a multiaxial fatigue framework, International Journal of Fatigue, 2010, 32 (12) : 1904-1912

S. Fouvry, H. Gallien, B. Berthel, "From uni- to multi-axial fretting-fatigue crack prediction: development of a stress-gradient-dependent critical distance approach", International Journal of Fatigue 62 (2014) 194–209

P. Arnaud, S. Fouvry, Modeling the fretting fatigue endurance from partial to gross slip: The effect of debris layer, Tribology International 143, 2020, 106 069

Wear models

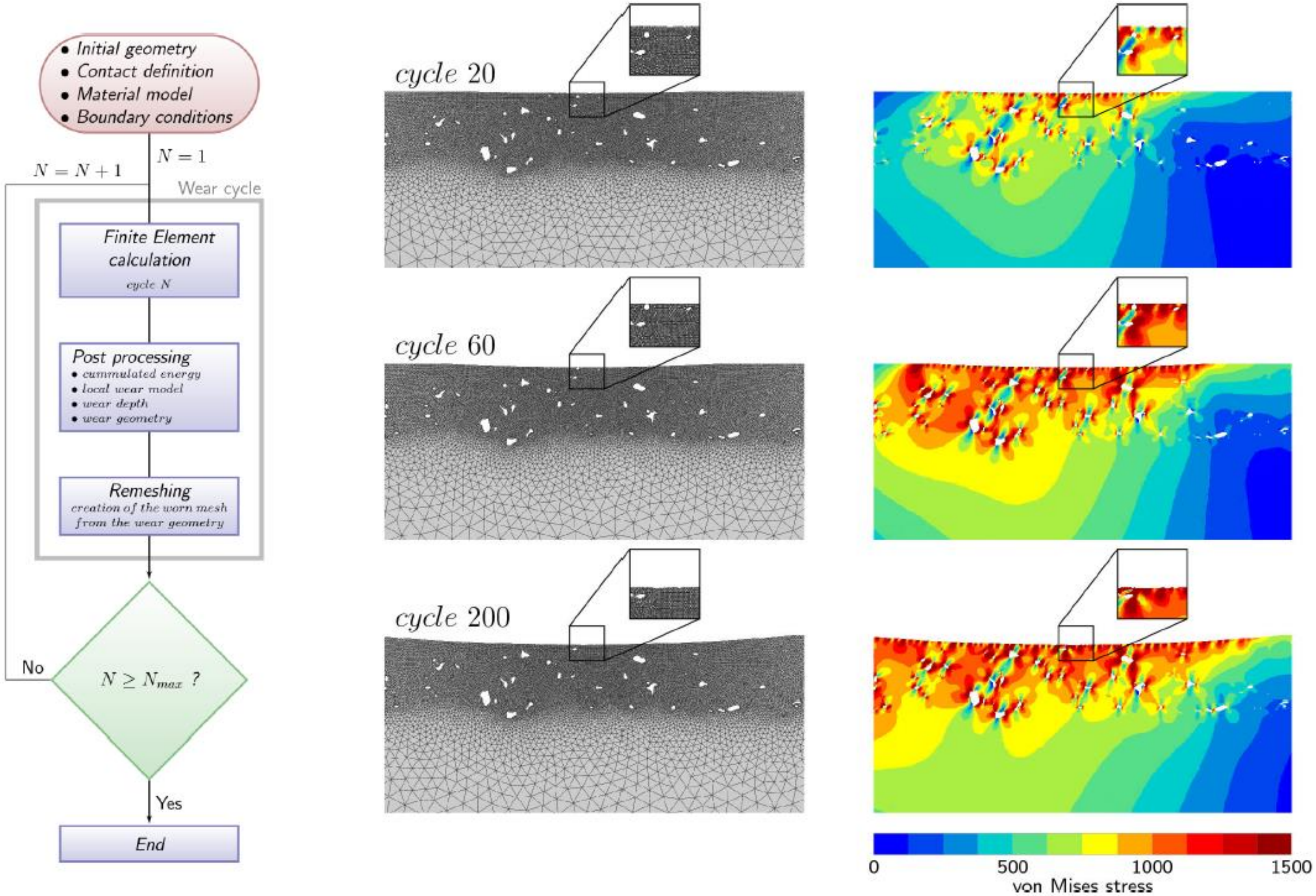

H. Proudhon *et al.*, Experimental and numerical wear studies of porous reactive plasma sprayed Ti-6Al-4V/TiN composite coating. *Wear*, (311) :159-166, 2014.

Crack propagation model (polycristal)

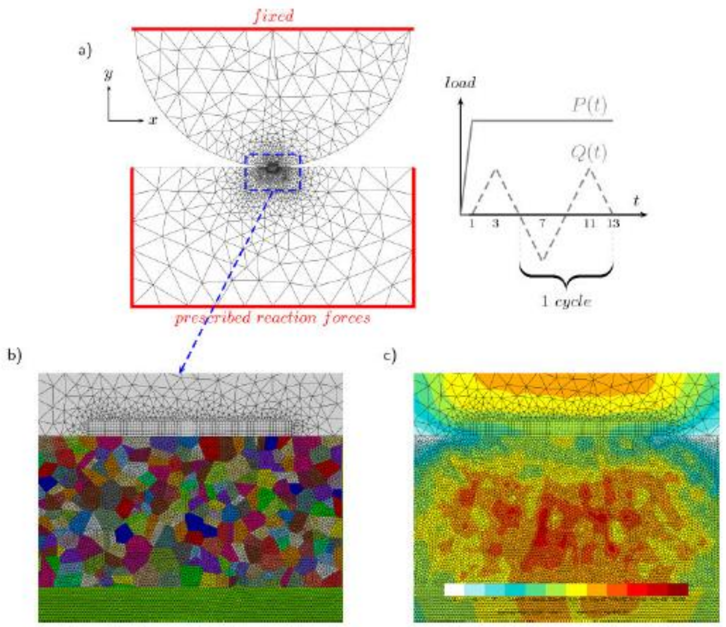

Crack initiation (fatigue criterion)

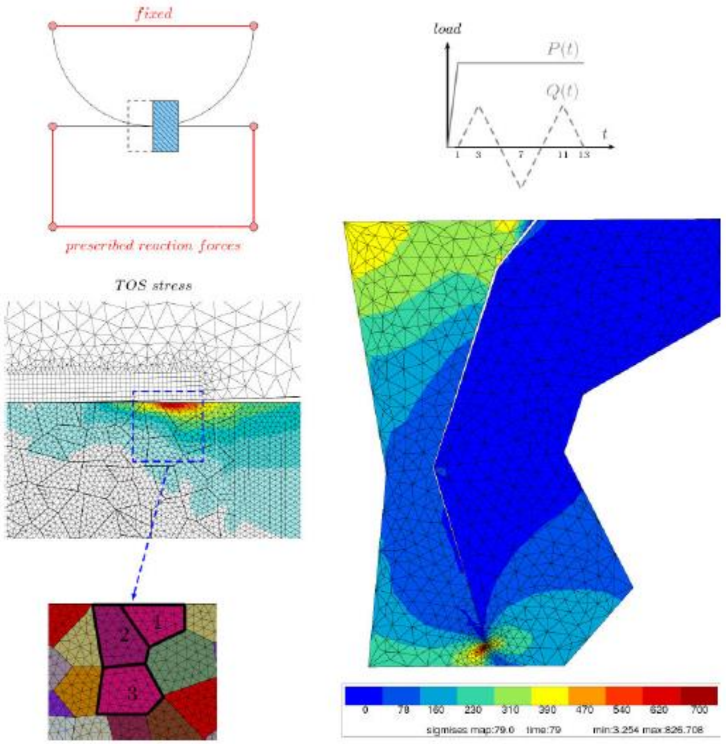

Crack propagation (crystal plasticity)

PhD thesis L. Sun (2012), H. Proudhon *et al.*, *Matériaux et Techniques*, (101) :203, 2013.